

SIGNAL PROCESSING OF SURFACE DETECTED
ELECTROMYOGRAPHIC ACTIVITY

SIGNAL PROCESSING OF SURFACE DETECTED
ELECTROMYOGRAPHIC ACTIVITY

by

John W.E. Whitman
B.Eng.Phys. (Dalhousie University)

A Thesis

Submitted to the School of Graduate Studies
in Partial Fulfilment of the Requirements
for the Degree.

Master of Engineering

McMaster University

July 1976

MASTER OF ENGINEERING
(Electrical Engineering)

McMaster University
Hamilton, Ontario

TITLE: Signal Processing of Surface Detected
Electromyographic Activity

AUTHOR: John W.E. Whitman
B.Eng.Phys. (Dalhousie University, 1973)

SUPERVISORS: Professors E. Della Torre and S.K. Sarna

NUMBER OF PAGES: xv, 104

To Helen Sarah

ABSTRACT

A technique is presented for assessing the relative performance of various signal processors of the surface detected electromyographic signal (EMG) in the gross skeletal muscles of man. A minicomputer is used to sample, store, and to later process the EMGs for agonists of the upper arm for various net forces, as measured at the wrist, under a condition of isometric tension. A two dimensional analysis of the flexor and extensor EMGs is performed for each force level. The number of force levels from which distinct, high confidence, control signals may be derived is used as a figure of merit to determine the superior of the signal processors studied and the superior of various electrode sites considered. For prosthetic use it is often desirable to maximize the number of control signals per muscle site.

ACKNOWLEDGEMENTS

The author wishes to thank his supervisors, Dr. E. Della Torre and Dr. S.K. Sarna, for their guidance and their many suggestions.

The discussions with H. deBruin concerning physiology and signal processing have been most fruitful. The assistance of K. Clark with certain programming problems is greatly appreciated.

Special thanks are due to my wife, Helen, who assisted me, not only with her encouragement, but also in many technical matters. Her help in preparing this thesis and its companion SOC report are most appreciated.

Credit is due to P. Dillon for her conscientious typing of this thesis.

TABLE OF CONTENTS

	Page
CHAPTER 1 - INTRODUCTION	1
CHAPTER 2 - PROPERTIES AND ANALYSIS OF THE EMG	5
2.1 Basic Physiology and Signal Properties	5
2.2 Traditional and Suggested Methods of Analysis of the EMG	7
2.3 Overall Aim and Experimental Procedure	14
CHAPTER 3 - MATHEMATICAL FORMULATION	25
3.1 Signal Processing Methods	25
3.1.1 Power Law Processors	25
3.1.2 The Peak Detector	29
3.1.3 Signal Processing Methods which Utilize the Peak Detector	31
3.2 Statistical Analysis	31
3.3 Determination of the Percentage of Data Points within an Ellipse	35
3.4 Discarding Ellipses	38
CHAPTER 4 - MEASUREMENT AND ANALYSIS TECHNIQUES	41
4.1 Data Acquisition	41
4.1.1 Electrodes and Amplifiers for the EMG	41
4.1.2 Positioning of Electrodes on the Upper Arm	46
4.1.3 The Force Transducer	48
4.1.4 Sampling and Storing of Signals	53
4.2 Computer Realization of the Various Signal Processors	56
4.3 Evaluation of Statistical Quantities	57

4.4	Determination of the Set of Ellipses to be Retained and the Percentage of Data Points within an Ellipse	61
CHAPTER 5 - RESULTS AND DISCUSSION		64
5.1	The Effect of Electrode Position on the Performance of, and the Relative Performance of, Signal Processors	64
5.1.1	Results	64
5.1.2	Discussion	69
5.1.3	Qualitative Observations on the Variation of the EMG with Wrist Pronation and Electrode Position	70
5.2	The Use of SNR's to Rank the Performance of Signal Processing Methods	74
5.3	Sensitivity of Parameters to Electrode Placement	75
5.4	Combined Data of Several Experiments	77
5.4.1	Results	77
5.4.2	Discussion	81
5.5	The Use of Rectangular Areas	90
5.6	One-Dimensional Analysis	93
CHAPTER 6 - CONCLUSIONS AND SUGGESTIONS		95
6.1	Conclusions	95
6.2	Suggestions for Further Work	99
REFERENCES		102

LIST OF FIGURES

<u>Figure</u>	<u>Title</u>	<u>Page</u>
2.1 (a)	Bi-phasic Surface Detected Action Potential	8
(b)	Surface Detected Electromyographic Signal	8
2.2	Muscles of the Upper Arm	15, 16
2.3	Graphical Representation of Statistical Parameters Associated with each Ellipse	19
3.1	Non-linear Analog Signal Processors	28
3.2	Flow Diagram of Peak Detector	30
4.1 (a)	Epoxy Encapsulated Amplifier and the Surface Electrodes	45
(b)	Electrode Positions	45
(c)	Positioning of the Flexor EMG Amplifier and the Ground Electrode	47
(d)	Positioning of both EMG amplifiers	47
4.2 (a)	Force Transducer	49
(b)	Position of Arm During Experimentation	49
4.3	Data Acquisition, Storage, Analysis and Display System	54
4.4 (a)	Plot of DISTILLED Data for SUM processor	60
(b)	Plot of Ellipses for SUM processor	60
5.1	Signal to Noise Ratios	72
5.2	SNRS at Various Force Levels	73
5.3	Combined Data for Several Electrode Positions	76
5.4	Combined Data for Several Experiments (0.5 second windows)	83
5.5	Combined Data for Several Experiments (1.0 second windows)	84

<u>Figure</u>	<u>Title</u>	<u>Page</u>
5.6	Plot of Solution Set of Ellipses.	85
5.7	Results for Normalized \overline{SUM}	86
5.8	Ellipses for Two Sampling Sequences	88
5.9	Ellipses for Two Experiments	88

LIST OF TABLES

<u>Table</u>	<u>Title</u>	<u>Page</u>
3.1	Signal-Processing Methods Employed	26, 27
4.1	Amplifier Specifications	44
4.2	Properties of the Force Transducer	50
4.3	Force Levels	52
5.1	Number of Levels as a Function of Electrode Position for Various Signal Processors (0.5 second data windows)	65
5.2	Number of Levels as a Function of Electrode Position for Various Signal Processors (1.0 second data windows)	66
5.3	Anatomical Data of Subject	67
5.4	Ranking of Processors using SNRS	72
5.5	Statistical Values for Combined Data for Six Experiments (Computer Print-out)	78, 79 80
5.6	Percentages and Levels for Six Experiments (Computer Print-out)	82
5.7	Number of Levels for Combined Data of Six Experiments	86

LIST OF ABBREVIATIONS

A/D	Analog to digital convertor
AMNAFF	Mean measured force for a force level
AP	Action potential
BB	Biceps brachii
BICEPS	Axis of DISTILLED data for flexor signal
BR	Brachialis
CMRR	Common mode rejection ratio
CRT	Storage oscilloscope computer terminal
D/A	Digital to analog convertor
DISTILLED	DISTILLED data refers to the values derived by processing the raw EMG
EMG	Surface detected electromyographic signal
FP	See Table 3.1
HP	See Table 3.1
Hz	Hertz
IRJECT	Number of windows of processed data rejected due to fluctuations in force
L1	A line in the BICEPS-TRICEPS plane along which the axis of an ellipse lies
MF	Muscle fibre
MU	Motor Unit
#LFT	Number of force levels left
QP	See Table 3.1
<u>PCC</u>	See Table 3.1
%AVG	Average percentage of points within the considered ellipses

%MIN	Minimum percentage of points within the considered ellipses
p.s.d.	Power spectral density
RAVG	See Table 3.1
RDOS	Real time disk operating system
RMS	Root mean square
SNR	Signal-to-noise ratio (See Page 12)
SUM	See Table 3.1
<u>SUM</u>	See Table 3.1
TRICEPS	Axis of DISTILLED data for extensor signal
TTY	Teletype

LIST OF MATHEMATICAL AND SPECIAL SYMBOLS

A	Semi-major axis of ellipse
A_{LPH3BN}	Measure of skewedness of tilted ellipse along line L1
A_{LPH4BN}	Measure of kurtosis of tilted ellipse along line L1
A_{LPH3TN}	Measure of skewedness of tilted ellipse along the ellipse axis normal to L1
A_{LPH4TN}	Measure of kurtosis of tilted ellipses along the ellipse axis normal to L1
A_{NGL1}	Angle formed by Line L1 and the BICEPS axis
A_{REA}	Area of an ellipse
B	Semi-major axis of ellipse
B_I	Value of DISTILLED data pertaining to the flexor
C_s	cosine of A_{NGL1}
$c(t)$	Modulation term of $E_{MG}(t)$
$E_{MG}(t)$	The EMG as a function of time
F	One-half the distance between the foci of an ellipse
F_D	Desired net force
F_{NOISE}	Noise threshold for peak detector
F_{PRES}	Present slope of $E_{MG}(t)$
F_{PREV}	Previous slope of $E_{MG}(t)$
F_r	Net force exerted
F_1, F_2	Foci of ellipse
F_{1BI}	Biceps axis coordinate of F_1
F_{1TRI}	Triceps axis coordinate of F_1

F_{2BI}	Biceps axis coordinate of F_2
F_{2TRI}	Triceps axis coordinate of F_2
I_{NB}	Number of samples per analysis window for digitized data
K	Sampling rate of $E_{MG}(t)$
$K_{FP}(i)$	Level number of first ellipse of the i th pair of overlapping ellipses
$K_{SP}(i)$	Level number of second ellipse of the i th pair of overlapping ellipses
L_1	Distance from data point to ellipse focus F_1
L_2	Distance from data point to ellipse focus F_2
M_{EANB}	Mean value of DISTILLED data over a force level for flexor
M_{EANT}	Mean value of DISTILLED data over a force level for extensor
N	Number of windows analyzed per force level
$n(t)$	Random component of $E_{MG}(t)$
N_{TCPT}	Intercept of TRICEPS axis with the line of linear regression to the data for a force level
P	A point having coordinates (B_I, T_{RI}) on the BICEPS-TRICEPS plane
P_E	Electrode position for monitoring the extensor EMG
P_{CC}	Number of peaks which exceed F_{NOISE} in an analysis window of $E_{MG}(t)$
$P(i)$	One condition which, if met, will ensure that no ellipses overlap
P_{TOP}	Peak-to-peak amplitude of $E_{MG}(t)$
P_{UFF}	Enlargement factor for ellipses
P_0, P_1, P_2, P_3	Electrode positions for flexors (Fig. 4.1(b))
r	Regression coefficient

S_{DVB}	Standard deviation of DISTILLED data for flexors
S_{DVBN}	Standard deviation of DISTILLED data along line L1 of ellipse
S_{DVT}	Standard deviation of DISTILLED data for extensor
S_{DVTN}	Standard deviation of DISTILLED data along the ellipse axis normal to line L1
S_{LOP}	Slope of linear least squares regression
S_N	sine of A_{NGL1}
T	Duration of analysis window
t	Time
T_{MAX}	The maximum of $E_{MG}(t)$ since the latest peak for which $P_{TOP} > F_{NOISE}$
T_{MIN}	A local minimum of $E_{MG}(t)$ used to calculate P_{TOP}
T_{RI}	Value of DISTILLED data pertaining to the extensor
V_{OFF}	Offset component of output voltage of force transducer
V_{OUT}	Output voltage of force transducer
(V_{XN}, V_{YN})	Coordinates of a point on an ellipse using the coordinate system of the axes of the ellipse
W	Weight of resting forearm
$X(i)$	i th sample of $E_{MG}(t)$
$x(t)$	$E_{MG}(t)$
$z(i)$	Differential input impedance of amplifier
ϕ_1	An angle in radians
ϕ_2	An angle in radians

CHAPTER I

INTRODUCTION

The surface detected electromyographic signal (EMG) of gross skeletal muscles is currently of considerable interest as a control signal for orthotic, prosthetic and environmental control devices. Superior processing of the EMG permits the realization of many distinct control functions from one muscle, thereby making efficient use of the muscle sites available.

For this reason, emphasis has recently been placed upon assessing the relative performance of existing signal processing techniques. Some of the major shortcomings apparent in much of the prominent research in this field, and in particular, in the work of Kreifeldt et al (5) and Hall et al (11), follow:

- (i) Analyses were performed with signal sequences of insufficient duration to obtain adequate representation of the statistical fluctuations in the processed EMG.
- (ii) The signal-to-noise ratio (SNR) in the processed EMG has been used alone to assess the relative performance of processors without any measure of the method's

sensitivity to changes in the EMG.

- (iii) Signals of low SNR (such as the rectified and smoothed EMG) have been presented to the subject as feedback when trying to maintain a constant level of muscle tension. Large fluctuations in the feedback signal prevent good controllability.
- (iv) In an agonist muscle pair, only the protagonist was considered, with the neglect of the antagonist.
- (v) No study was conducted on the effect of electrode position on the quality of the results.
- (vi) Signal processor performances were compared with different EMG sequences presented to each processor.

This thesis along with an internal technical report (16), describes our approach to experimentation and analysis of the EMG. The aim was to develop a technique which could be used to assess the performance of several signal processors and to study the effect of electrode position on results. A minicomputer was used for sampling and storage of the EMG's of the flexor and extensor muscles of the upper arm under isometric contraction. The subject maintained as constant a net force as possible. The net force was measured at the wrist with the elbow resting and held at angle of 90° .

The signal was broken into successive 0.5 second windows for analysis. The values of the processed signal were considered in a two dimensional coordinate system for cluster analysis. One axis represented the processed flexor

values while the other indicated the extensor values. The statistical parameters of the processed values for each of twenty-three different net forces (force levels) were assessed. From these parameters, isoprobability ellipses were constructed in the plane. The ellipses were allowed to enlarge in unison. The number of distinct, definable ellipses was found by using two conditions. The first was that one ellipse of each overlapping pair must be discarded. The choice of which ellipse to discard was made so as to retain the largest number of distinct ellipses. The second condition was that the measured percentage of processed data enclosed by the appropriate ellipse averaged at least 95% over all non-discarded ellipses. The electrode position and the signal processing method which permitted the largest number of non-overlapping ellipses were chosen as superior.

In our procedure and analysis, an attempt was made to minimize as much as possible the difficulties previously described. The measures employed to overcome these problems follow:

- (i) The analysis programs allowed the consideration of eleven experiments simultaneously. Each experiment could consist of a maximum of twenty-three force levels with twenty seconds of signal sampling per force level. Thus as much as 220 seconds of EMG per force level could be considered at once. This corresponds to 440 windows of 0.5 seconds duration or 440 processed values for use in statistical analysis. Programs are easily upgradable

to consider more than eleven experiments.

- (ii) The number of distinct, definable ellipses was used to assess processor performance. This value depended on both SNR and on the sensitivity of the processed values to changes in EMG.
- (iii) For each desired net force, the deviations of the force from this value were monitored by a force transducer. This signal, having a high SNR, was presented to the subject as visual feedback by using an oscilloscope. Using this technique, force was controllable to within $\pm 2\%$ of the desired value.
- (iv) Flexors and extensors were simultaneously considered.
- (v) Several electrode positions for the flexor signal were studied. It was considered crucial to examine this for the flexor signal since forearm flexion is achieved by the use of two distinct muscles rather than one (Section 5.1.3).
- (vi) Since the sampled signal was stored on disk, it was possible to apply an identical signal to each of the eleven signal processors which were realized in software.

Due to the ease with which they can be implemented, rectangular regions were studied as an alternative to ellipses. Also, the number of distinct levels definable for a one dimensional case, where only the extensor EMG is considered, was investigated.

CHAPTER 2

PROPERTIES AND ANALYSIS OF THE EMG

2.1 Basic Physiology and Signal Properties

The gross skeletal muscles of man consist of many individual muscle fibres (MF) each capable of contracting upon stimulation [1]. A MF is stimulated by a complex neural network involving the central nervous system. Activation by a signal from the nervous system initiates a chemical process in the MF involving the release of potential energy stored in the form of ionic concentration gradients at the muscle fibre's cell walls. A transport of ions across the cell membrane of the MF occurs during activation.

This transport of ions first commences at the innervation point of the MF and then propagates at a velocity determined by many factors down the length of the long rod-like MF resulting in a propagating wave of depolarization. The varying electric field associated with this wave of depolarization is referred to as an action potential (AP). An AP is electronically detectable both intra- and extra-muscularly. This varying electric field induces certain protein molecules of the fibrils of the MF to move in such a fashion as to cause a shortening in the overall fibre length, giving rise to the force of contraction. Many MF's are innervated by a common

nerve and respond in unison to stimuli. Such a group of fibres is referred to as a "motor unit" (MU) and is the smallest unit of the muscle which may be controlled independently.

A muscle is composed of many such motor units. These MU's are activated in an asynchronous manner in order to achieve the desired net muscular force. The two main mechanisms by which different muscular tensions are achieved are the recruitment pattern of MU's and their firing rate.

In a muscle, there is a graduation in the threshold force at which different MU's will be recruited and in the twitch tension produced by these different MU's. Those recruited at higher thresholds exhibit higher twitch tensions than those recruited at lower thresholds [2]. The effect of the MU recruitment pattern on net muscular force is greater at lower force levels than at higher ones since, for higher force levels, the individual thresholds of most MU's have been exceeded and they are already active. It is the increase in firing rate of MU's at higher force levels which is primarily responsible for the muscle's activity [2].

To monitor the electrical activity intramuscularly fine wire or needle electrodes are often used. Due to their small size, these electrodes are selective in nature and can monitor the activity of a few muscle fibres. Milner-Brown et al [2] have studied the properties of the surface potential in relation to muscle physiology by using needle electrodes for intra-muscular recording and large area surface electrodes

for extra-muscular recording. Great interest exists in this surface potential or surface detected electromyographic signal (EMG) since it is readily available and can be useful in diagnosis or as a control signal for prosthetics. From their studies of certain muscles of the hand, Miner-Brown et al determined that the MF's comprising a MU are scattered throughout a volume of the muscle rather than localized in a bundle as was once believed. They also found that MU's of different activation thresholds are located uniformly throughout the muscle.

2.2 Traditional and Suggested Methods of Analysis of the EMG

A photograph of a bi-phasic surface detected AP is shown in Fig. 2.1(a). We photographed this AP from a storage oscilloscope trace of the EMG of the biceps at a low force level. The EMG consists of the summation of many such wave forms. Fig. 2.1(b) is a sample of the EMG as measured from the biceps muscle at a moderate level of contraction. The activity of the antagonist (triceps) is also shown. In both measurements, the apparatus and electrode positions were as described in Section 2.3, and Chapter 4.

In an attempt to discover a superior method of signal processing of the EMG, a wide variety of techniques have been employed with the goal of maximizing some or all of the following properties:

- (i) Long term reproducibility
- (ii) Short term stability

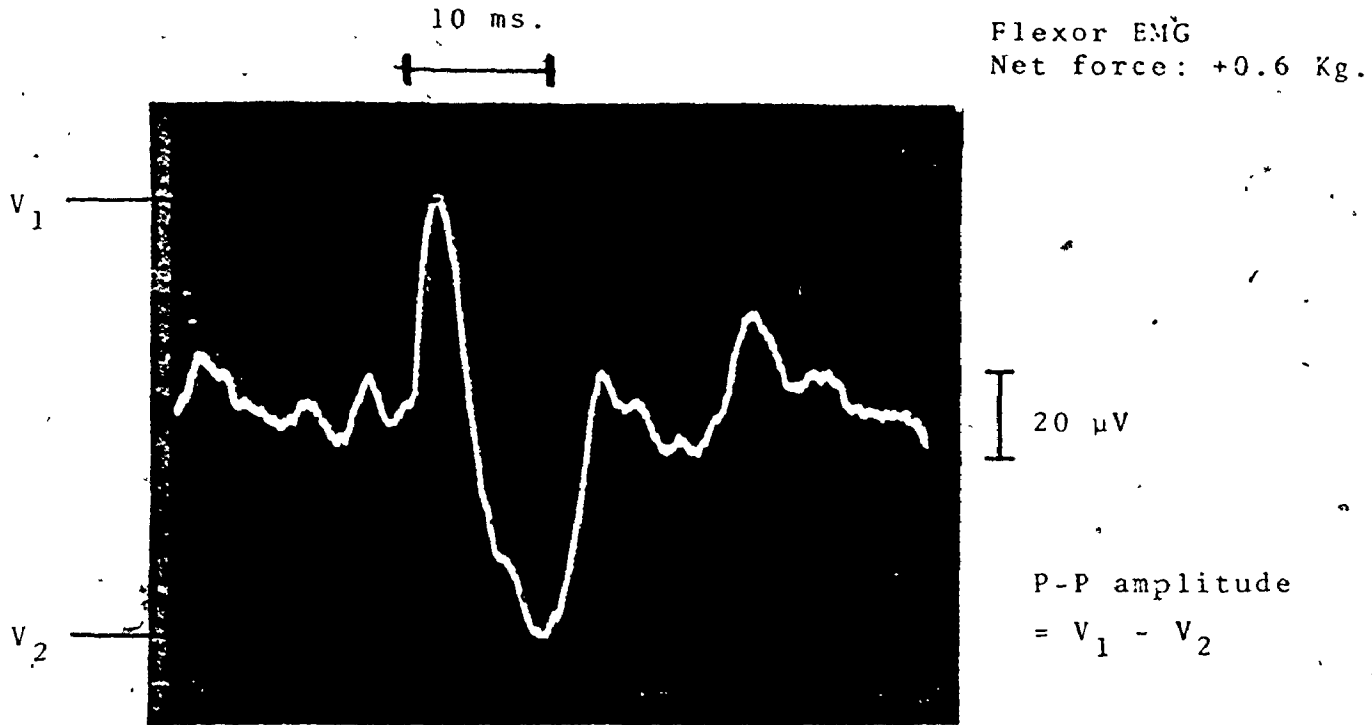


Fig. 2.1(a) Bi-phasic Surface Detected Action Potential

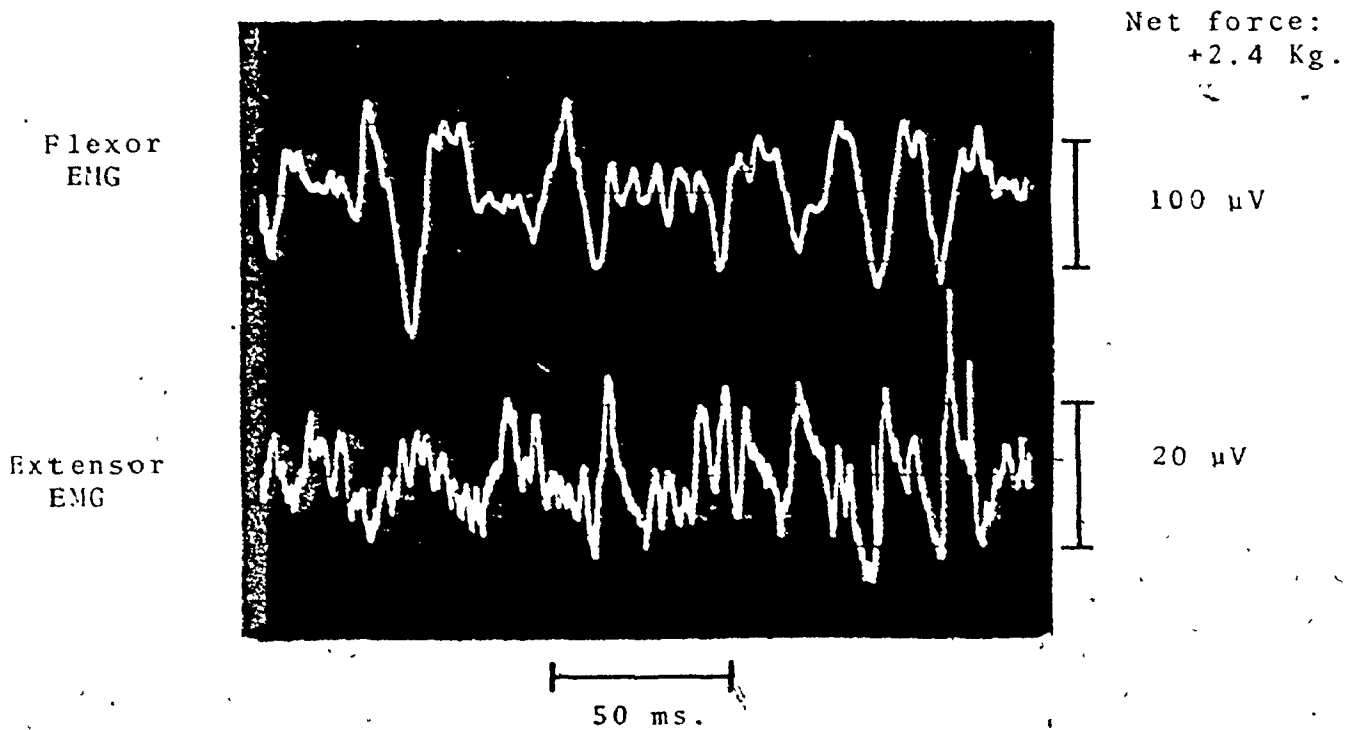


Fig. 2.1(b) Surface Detected Electromyographic Signal

(iii) Sensitivity of processed signal to changes in the level of muscle tension.

Superior signal processing allows the processed signal from a muscle site to be used either for discrete multi-function control, or to be used for proportional control of prosthetic, orthotic and environmental control devices.

Although many experimenters have considered that the duration of an action potential may vary as a function of the tension generated by the MU, Milner-Brown et al [2] observed no such trend experimentally. They argued that their observations, supported by anatomical studies, indicate that motor units of higher twitch tensions do not possess more, but rather larger, MF's. It has been reported [3] that the rate of zero crossing of the EMG bears no marked relationship to force. Since others (deBruin, private communication [4]) have had success with peak counting techniques and since our early investigations revealed them to be poor, but not without merit, we also studied these techniques. In a peak counting method only peaks of a peak-to-peak (P-P) amplitude in excess of a threshold, which is determined by the noise in the measurement system, need be considered. When AP's summate they may produce an effective offset in the EMG baseline over short periods of time. A zero crossing technique provides poor results in such an instance whereas a peak counting technique is less severely effected.

An approximate mathematical representation of the EMG has been suggested [5] where the activity ($E_{MG}(t)$) consists

of an amplitude modulated noise signal:

$$E_{MG}(t) = c(t) n(t) \quad (2.2.1)$$

where $c(t)$ is the modulation term and

$n(t)$ is the noise or carrier signal.

The modulation term $c(t)$ is related to the level of muscular tension and contains useful information to be recovered by signal processing.

By applying such techniques as signal rectification and low pass filtering, it is possible to retrieve some useful information since $c(t)$ has components of lower frequency than $n(t)$. This is particularly true for the situation, of primary interest in this study, where the subject uses closed loop central nervous system control (such as visual feedback) for voluntary exertion in the large skeletal muscles, such as the biceps and triceps.

Many experimenters have observed that the muscular force and the EMG, which has been processed by rectification and averaging (RAVG), are linearly related. In such experiments, various muscular tensions are investigated with the subject maintaining as constant a tension as possible. Until recently a successful explanation of this relationship has been elusive. Milner-Brown et al [2] have elucidated this situation by suggesting that the linearity is due to the exact nature of the contributions of recruitment and firing rate of the MU's to the EMG. They were able to isolate and examine individual action potentials. They observed that the P-P amplitude (Fig. 2.1) is linearly related to the area

under the wave form. The sum of such P-P amplitudes (SUM) should therefore be related to the RAVG by a simple constant.

Since the P-P transition occurs in a fraction (0.3 to 0.5) of the total AP duration and since the P-P amplitude is independent of any base line, SUM is less sensitive to any frequency components of base line drift which are within the amplifier's bandwidth, than is RAVG. Furthermore, at higher force levels, the increase in MU firing rate and the increase in the number of active MU's, due to the recruitment pattern, causes an increased probability that individual AP's will overlap each other in time. This results in a decrease in the information concerning muscular contraction which is retrievable from the EMG, since it consists of the summation of many AP's. As the time interval involved in measurement of P-P amplitude is only a fraction of the total AP duration, the probability that AP's will overlap during a P-P transition is less than the probability that they will overlap at all. Hence the P-P amplitude is less likely to be strongly effected by overlap than is RAVG. For these reasons, SUM should prove to be a more reliable measure of muscular contraction than RAVG, particularly at higher force levels.

The EMG has a random component ($n(t)$) and since it exhibits only short term stationarity, the type and time constant of the filter used helps to determine the reliability of the results. The work of Kreifeldt [7] demonstrates that of first and third order Butterworth and of third order averaging filters, the averaging filter is superior. As will

be discussed shortly, the experimental method used in his assessment of filters causes the results to be difficult to interpret. Since we wished to use a digital computer for analysis, it was decided to use the easily realizable averaging filter.

Kinesthetic studies performed by Neilson [6], having the goal of tracking imposed random angular changes in the subjects other arm, indicate that, for voluntary control of the elbow angle, the significant spectral power is only in the 0-2 Hz. band of frequencies. Since we were interested in muscles which control elbow angle and we wished to find a signal processing method providing a signal suitable to control tasks of a voluntary rather than a reflex nature, it was decided, having considered Neilson's results, that a filter time constant of 0.5 seconds would allow a sufficiently rapid system response. In addition, a 1.0 second filter time constant was utilized to note the degree of improvement of results as a function of the filter time constant.

The RAVG has been used with some success by several experimenters. Dorcas and Scott [8] [9] have produced and clinically tested a three-state myoelectric control system. Bottomley [10] presents a scheme where both the protagonist and antagonist muscles of an agonist muscle pair are considered for control purposes. Kreifeldt et al [5] gives a mathematical formulation to predict the signal (the mean value) to noise (the standard deviation) ratio (SNR) of several classes of non-linear signal processors including the RAVG processor

for the case where muscle tension is constant. This is done to determine the superior processor from the point of view of SNR. The SNR's predicted on the basis of Kreifeldt's formulation and those which he observed were markedly different.

One of the main reasons for this difference may be that in the formulation, it was assumed that the muscular tension ($c(t)$) was a constant while the experimental arrangement did not ensure this. To assist the subject in maintaining a constant tension, Kreifeldt presented the smoothed EMG as feedback. When a rectified EMG is smoothed by a filter of short time constant, statistical fluctuations of significant amplitude will be present in the output signal and the output signal will not be an accurate measure of the muscular contraction level at each instant. The use of such noisy signals for feedback will make it difficult for the subject to maintain $c(t)$ constant and it is possible that he will produce large oscillations in $c(t)$. In his formulation, Kreifeldt assumed that $n(t)$ may be represented as Gaussian noise whereas recent results [2] indicate that this is not necessarily true. Others [11] utilized the same form of feedback and found similar SNR (i.e. SNR \approx 2 to 4) when performing a study of the biceps-triceps muscle pair.

Although the use of the net force for feedback is far superior to the use of smoothed EMG, a constant net force does not imply a constant level of muscular tension in an agonist muscle pair. This is because the net force is the

difference between the force exerted by each agonist. Some experimenters have monitored the antagonist's activity and have accepted only signal sequences in which this activity is below an acceptable minimum. The author has found that the EMG for the antagonist muscle is usually too high to ignore. This may be due to antagonist activity or the detected signal may arise from the activity in the adjacent protagonist. Without the aid of needle electrodes to selectively monitor activity, it would be incorrect to assume that the antagonist is inactive.

For the upper arm, it is difficult to isolate the contributions to the EMG of individual muscles. The biceps brachii (BB) and the brachialis (BR) are both active during isometric contraction with the wrist supine. Due to their proximity, considerable cross-talk may exist in the EMG. The primary extensor of the forearm about the elbow is the triceps. This muscle consists of three different heads, each active under certain circumstances but all active during extension against a resistance [13]. From the complexity of the situation; it is to be expected that electrode position, in part, determines the quality of results. An illustration of these muscles is given in Fig. 2.2.

2.3 Overall Aim and Experimental Procedure

A set of experiments was designed to provide the following information:

- 1) the performance of several signal processors.

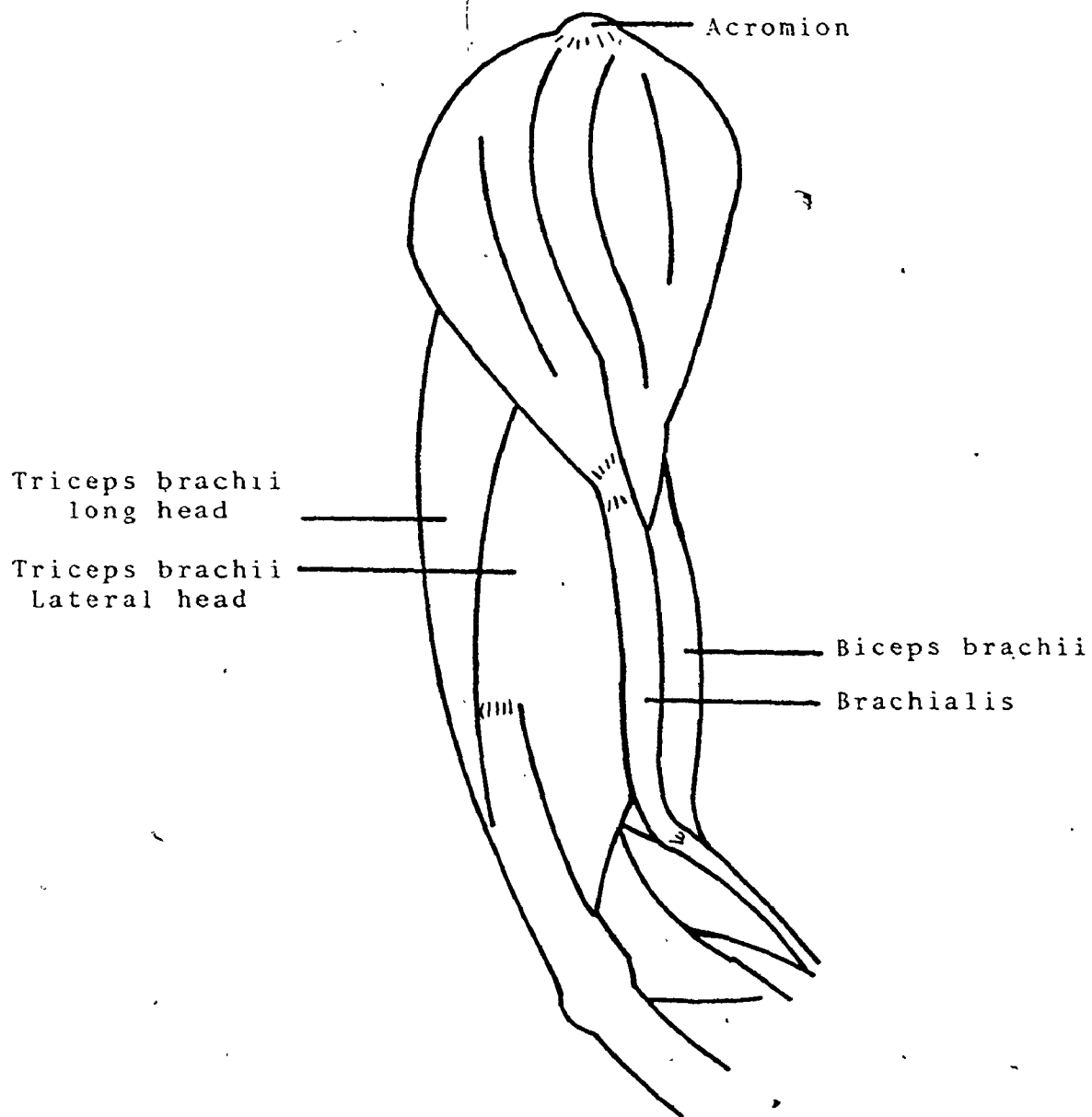


Fig. 2.2 Lateral View of muscles of Upper Arm

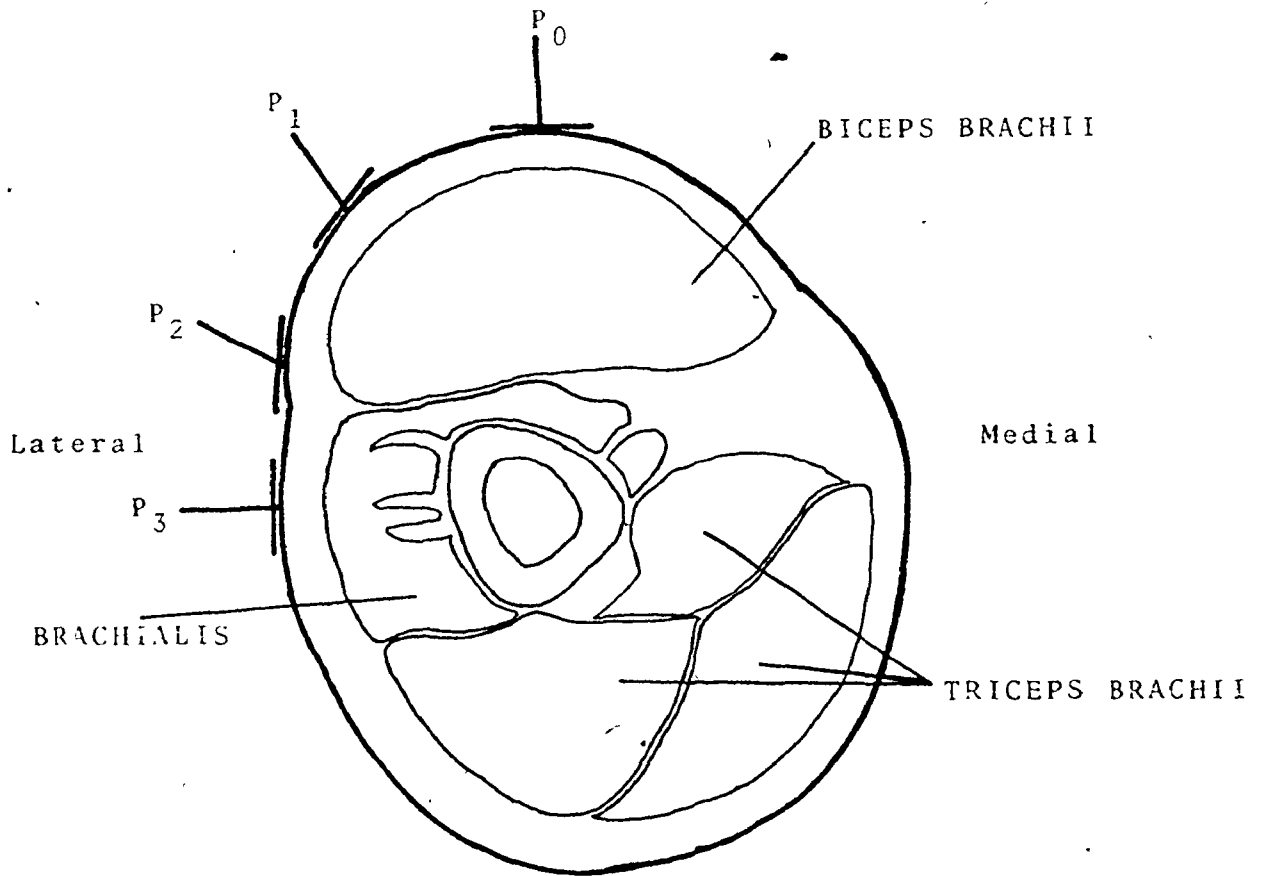


Fig. 2.2 (cont'd) Cross Section of Upper Arm

- 2) the effect of electrode position on the quality of the results.

The necessary hardware and software were developed (Chapter 4), [16]. Due to a lack of time it was impossible to perform exhaustive experimentation or to perform experiments on more than one subject.

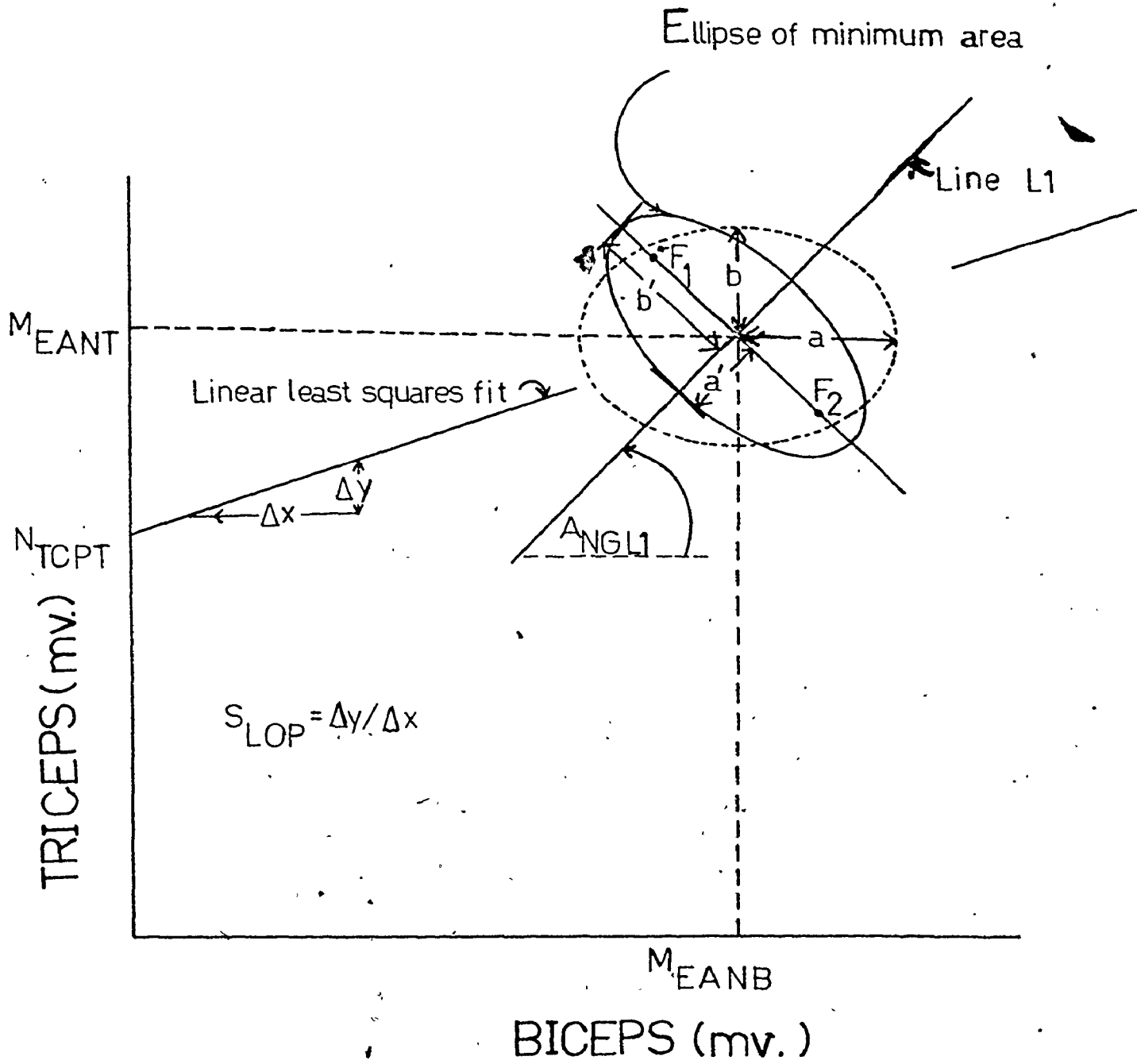
Our study was of the EMG of the muscles of the upper arm in a condition of isometric contraction. To maintain as constant a torque as possible about the elbow joint, visual feedback, related to the net force as measured at the wrist, was used. The force transducer has such a high SNR that the statistical fluctuations in the output due to noise are small compared with the actual fluctuations in force. Thus it is a reliable signal to use for feedback. This eliminates the problems encountered when signals of a low SNR, such as the rectified and smoothed EMG, are used for feedback. The negligible time constant of the force transducer, with respect to the frequencies of interest, ensures that, unlike some signals, such as the processed EMG, the feedback signal is in-phase with the variable which is to be controlled.

With the net force as constant as possible the EMG of both the flexors and of the extensors was monitored using two small, source attached (i.e. physically near the surface electrodes), high gain, differential input instrumentation amplifiers. With the aid of a NOVA 830 minicomputer equipped with an A/D unit, disks and supporting RDOS (Real-time Disk Operating System), large scale signal sampling and data storage

was possible. Each experiment consisted of several ten second intervals during each of which the subject exerted a constant force at some particular level while both of the EMG signals and the force transducer signal were sampled. The range of forces used was approximately -8.0 to $+10.0$ Kg where a negative force extended the forearm and a positive force flexed it. One great advantage of storing data is that the relative performance of the various signal processors can be assessed utilizing identical input signals. Further information concerning the apparatus and experimental procedure is presented in Chapter 4.

Each EMG signal was processed separately, thereby producing a pair of values for each successive 0.5 second period (window) for a particular processing technique. These values are referred to as "DISTILLED" data. The value pertaining to the flexors is referred to as " B_I " (biceps) and that pertaining to the extensors as " T_{RI} " (triceps). By considering these values as coordinates in a plane, clusters of data associated with each force level can be obtained.

This two dimensional approach immediately suggests the use of bivariate statistical analysis as a means of defining suitable areas on the plane to enclose clusters of data. For a normal distribution, the two-dimensional mean and the standard deviations about the mean in each dimension may be used to construct isoprobability ellipses [12] in the plane for each force level. In Fig. 2.3 such an ellipse is illustrated in dashed lines. The mean of the B_I data is



$a : S_{DVB}$ $b : S_{DVT}$ $F_1 \text{ \& } F_2 : \text{foci}$
 $a' : S_{DVBN}$ $b' : S_{DVTN}$

Fig. 2.3 Graphical Representation of Statistical Parameters Associated with each Ellipse

referred to as " M_{EANB} " while that for the T_{RI} data is " M_{EANT} ". The standard deviation about the mean of the B_I data is " S_{DVB} " while that for the T_{RI} data is " S_{DVT} ". The axes of the ellipse are drawn parallel to the coordinate system's axes and each are two standard deviations in length. The probability that a given data point lies within the ellipse associated with the particular force level is 68%.

To maintain a constant force when the antagonist muscle increases tension, the protagonist must increase its activity. These changes will be evident in the DISTILLED data and cause a simultaneous increase of both M_{EANB} and M_{EANT} . This increase may not be linear. In such a situation, it is possible to define another ellipse with an axis along a line intercepting the BICEPS axis at some angle (A_{NGL1}) which has a distinctly reduced area as compared with the previously defined ellipse. This situation is illustrated in Fig. 2.3. The line $L1$ is one axis of this new ellipse while a line perpendicular to it, passing through the two dimensional mean, is the other axis. The standard deviation measured along $L1$ is " S_{DVBN} " while that measured along the other axis of the ellipse is " S_{DVTN} ". In addition, it is possible to choose A_{NGL1} so as to minimize the ellipse area. Further information and the mathematical relationships defining these statistical parameters are presented in Chapter 3.

The use of statistical parameters to define suitable regions to enclose data clusters and the use of the ellipse of minimum area provide two advantages. Results are easy to

interpret and excessive development time is not necessary since calculations are comparatively uncomplicated. Considerable complexity would be involved if regions of a general shape were used.

For reasons to be discussed in Chapter 5, the measured distributions are often not normal. However, if the data for different experiments may be assumed to be statistically independent, the distribution will approach a normal one when the results of a large number of experiments are combined. For this reason, it was decided to measure certain parameters associated with the higher moments of the distribution. These parameters are described in Chapter 3. A linear regression to the data was also performed and the regression co-efficient (r) was calculated. When $|r| \approx 1$, the data has a marked linear trait. In such a case the linear fit is useful in determining how M_{EANB} and M_{EANT} vary, at constant force, for different muscle contraction levels. We did not have time to investigate this variation, but certain suggestions are made (Section 6.2) concerning this.

If a distribution is not normal the probability of the data lying within the appropriate ellipse of a given size (where size refers to its axes dimensions measured in units of S_{DVBN} and S_{DVTN}) is difficult to assess. It also implies that ellipses are not necessarily isoprobability surfaces. Because of this, it was necessary to count the percentage of data points actually lying within an ellipse to obtain a measure of the confidence.

If an ellipse is enlarged, a higher percentage of

data points will lie within it. All ellipses were allowed to enlarge in unison and overlapping ellipses were discarded in order to retain as many distinct regions as possible with the restriction that as high a reliability as possible was maintained.

Based upon the above considerations, a criterion was established by which the relative performance of the various signal processing methods could be assessed. The superior signal processing method was chosen as the one which permitted the definition of the largest number of distinct ellipses with the condition that the average percentage of DISTILLED data points within these ellipses be greater than 95%.

This was considered to be a useful criterion for assessing the performance of the signal processing methods since the definition of many distinct levels permits the realization of many unique control functions from one muscle pair. It has been argued that it is inefficient to use both agonists in one control unit since this prohibits the independent use of each for simultaneous control of two functions. Developing independent muscle control requires more training whereas in our method, in which the subject exerts a desired net force, natural muscle usage is maintained. Also, as we have observed (Section 5.6) more distinct control levels are definable using the proposed two-dimensional scheme, than by considering the agonists independently.

Although many experimenters (5) (11) have noted the importance of the SNR in assessing the performance of signal

processing techniques, the sensitivity of the various methods should also be considered. The above procedure incorporates both of these features. Examination of the SNR in our experimentation revealed whether or not the SNR, in itself, provided a useful parameter with which the relative performance of signal processors may be examined (Section 5.2).

It was decided to employ data filtering windows of both 0.5 and 1.0 seconds and to examine a total of eleven different processing methods. The various power and some of the root law detectors examined by Kreifeldt [5] were included in the study. As was mentioned earlier, the method of peak counting was also of interest. Method SUM, applied to both the signal and the inverted signal, was investigated. It was necessary to examine both the signal and the inverted signal to ascertain if a superior performance is obtained for one of them using the peak detecting method as described in Chapter 3. It was also decided to evaluate the performance of a series of methods where the sum of a power of the P-P amplitude is determined over each data window. Further discussion of the signal processing methods studied is given in Chapter 3 and a summary of these methods is given in TABLE 3.1.

Due to time limitations it was not possible to study other promising signal processing techniques of recent interest. The potential of time series analysis techniques has been demonstrated by Graupe et al [14]. A simple technique differentiating between muscular actions for adjacent muscles

with high cross-talk by considering signal phase has been described (15).

CHAPTER 3

MATHEMATICAL FORMULATION

3.1 Signal Processing Methods

Eleven different signal processing methods are considered in this study. These methods and their mathematical definitions are presented in Table 3.1. The following observations and definitions should help to clarify the information found in this table.

3.1.1 Power law processors:

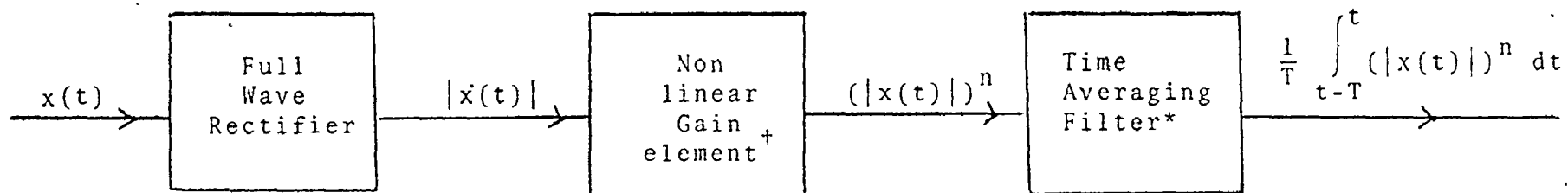
A total of five power law signal processors were examined. Analog equivalents of these processors would consist of a full-wave rectifier followed by a non-linear gain element followed by an averaging filter. This is illustrated in Fig. 3.1. The signal $x(t)$ is first rectified providing an input of $|x(t)|$ to the non-linear gain element. The output of this non-linear gain element is $(|x(t)|)^n$. The ideal averaging filter, as indicated in Fig. 3.1, produces an output which is the time average of its input signal over the interval T . Such a processor may be realized on a digital computer utilizing a high level language such as FORTRAN with minimal effort.

Table 3.1 Signal processing methods employed

METHOD NUMBER	DESCRIPTION	MATHEMATICAL DEFINITION	ABBREVIATED NAME	APPLIED BY PROGRAMS:
1	Sum of all peak to peak signal excursions over a window which exceed F_{NOISE}	$P_{\text{CC}} \sum_{i=1} (P_{\text{TOP}}(i))$	SUM	DISTILL
2	Rectified average of signal	$\left[\sum_{i=1}^{I_{\text{NB}}} x(i) \right] / I_{\text{NB}}$	RAVG	DISTL2, DISTL5
3	Average of fourth power of signal.	$\left[\sum_{i=1}^{I_{\text{NB}}} (x(i))^4 \right] / I_{\text{NB}}$	FP	DISTL5
4	Average of second power of signal.	$\left[\sum_{i=1}^{I_{\text{NB}}} (x(i))^2 \right] / I_{\text{NB}}$	SP	DISTL5
5	Average of half power of rectified signal.	$\left[\sum_{i=1}^{I_{\text{NB}}} (x(i))^{1/2} \right] / I_{\text{NB}}$	HP	DISTL5
6	Average of quarter power of rectified signal.	$\left[\sum_{i=1}^{I_{\text{NB}}} (x(i))^{1/4} \right] / I_{\text{NB}}$	QP	DISTL5
7	Same as #1 but as applied to inverted signal.	$P_{\text{CC}} \sum_{i=1} (P_{\text{TOP}}(i))$	$\overline{\text{SUM}}$	DISTL5

Table 3.1 (continued)

METHOD NUMBER	DESCRIPTION	MATHEMATICAL DEFINITION	ABBREVIATED NAME	APPLIED BY PROGRAMS:
8	Count of all peaks of height > F_{NOISE} for the inverted signal.		\overline{PCC}	DISTL5
9	Sum of the square of peak to peak signal excursions for the inverted signal.	$P_{CC} \sum_{i=1} (P_{TOP}(i))^2$	\overline{SMSP}	DISTL5
10	Sum of the peak to peak signal excursions raised to the power of 3/2, for the inverted signal.	$P_{CC} \sum_{i=1} (P_{TOP}(i))^{3/2}$	$\overline{SMIP5}$	DISTL5
11	Sum of the peak to peak signal excursions raised to the power of 1/2, for the inverted signal.	$P_{CC} \sum_{i=1} (P_{TOP}(i))^{1/2}$	\overline{SMHP}	DISTL5



† Logarithmic and anti-logarithmic amplifiers are used to produce the desired transfer function [5].

* H. Garland

"A State Variable Averaging Filter for Electromyogram processing."
Med. & Biol. Eng., Vol. 10, pp. 559-560;
 (1972).

Fig. 3.1 Nonlinear analog signal processors

For digitized data, the input to the processor is a series of distinct samples $(X(i))$ taken over a measurement window of length T seconds at a sampling rate of K samples/second. Thus, for one data window, a total of I_{NB} samples are recorded where:

$$I_{NB} = TK \quad (3.1.1)$$

Using digitized data, a power law processor, of power n , which performs the same function as the previously described analog processor, does so by evaluating:

$$\frac{1}{I_{NB}} \sum_{i=1}^{I_{NB}} (|X(i)|)^n \quad (3.1.2)$$

The mathematical definitions of the various power law processors which we studied are given in TABLE 3.1.

3.1.2 The Peak Detector:

A short FORTRAN routine designed to detect peaks and determine the peak-to-peak amplitudes was adapted from one written by deBruin (private communication (4)). This peak detector monitors the slope of the signal for changes. When a change of slope occurs the sequences of events depicted in the flow diagram (Fig. 3.2) ensues.

Initially, the value of the previous slope (F_{PREV}) and the value of the previous maximum (T_{MAX}) are zero. This peak detector searches for a positive peak or plateau which represents a local maximum that is greater than the current T_{MAX} . When a minimum is found (T_{MIN}) such that the P-P amplitude (P_{TOP}) is greater than a previously determined noise

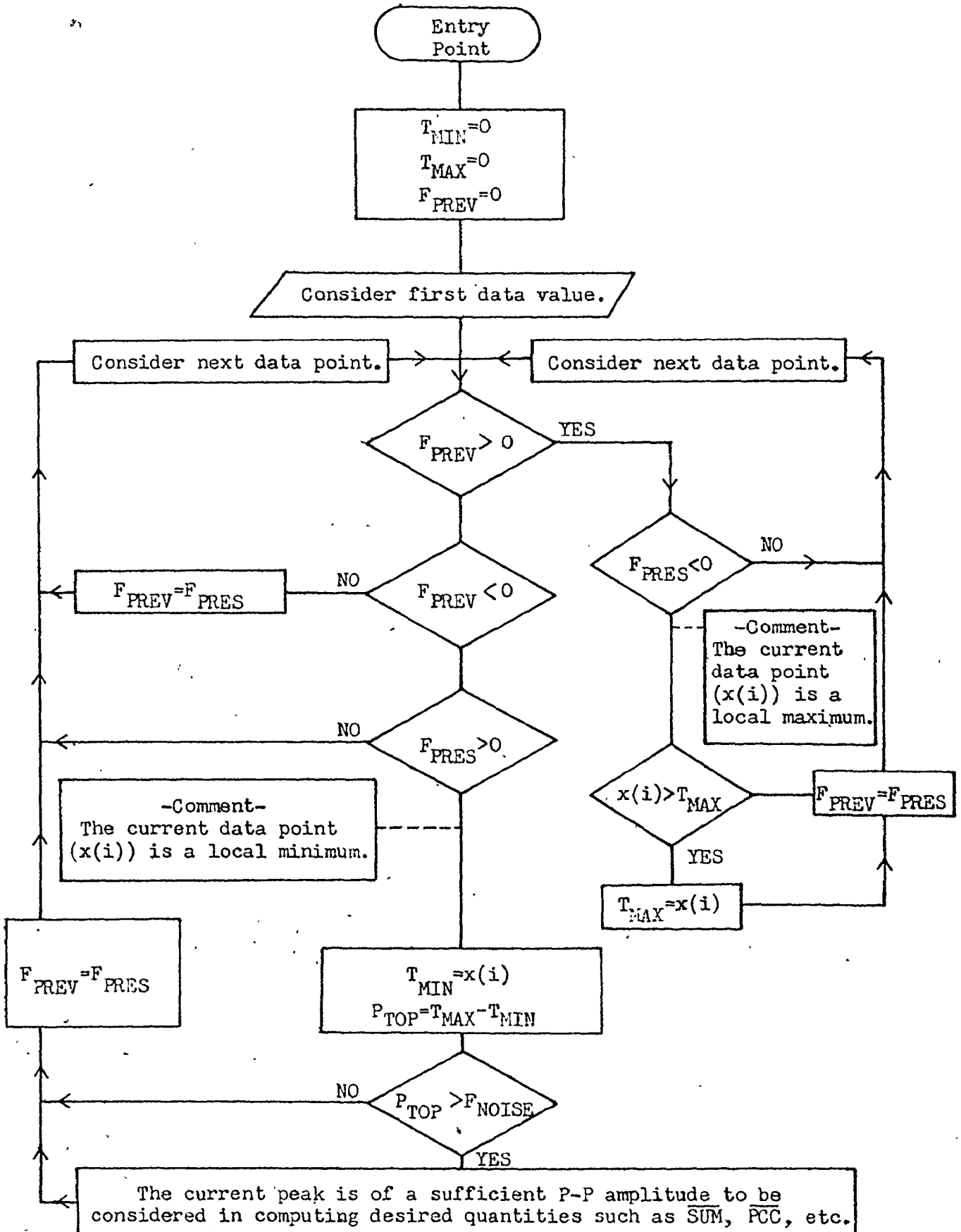


Figure 3.2 Flow Diagram of Peak Detector

threshold (F_{NOISE}), the peak is considered to be of significant amplitude. The P-P amplitude is:

$$P_{\text{TOP}} = T_{\text{MAX}} - T_{\text{MIN}} \quad (3.1.3)$$

If P_{TOP} is greater than F_{NOISE} , the value of the data point currently under consideration, which in this case is a local minimum, is assigned to T_{MAX} . This assures that the next value of T_{MAX} will be that of the next local maximum even though this maximum is less than the value of T_{MAX} used in calculating the previous value of P_{TOP} .

3.1.3 Signal Processing Methods which utilize the peak Detector:

Method SUM is simply the running sum, over the window of interest, of all of the P_{TOP} values which are of significant amplitude. The total number of such peaks in a window is the peak count (P_{CC}). To investigate the effect of inverting the signal, the running sum of all of the P_{TOP} values over the window of interest was also evaluated for the stored values after negation ($\overline{\text{SUM}}$). Refer to TABLE 3.1 for information on these, and on other, peak detecting methods.

3.2 Statistical Analysis

Analysis of a bivariate distribution reduces to two one-dimensional problems. The notation and the particular form of the equations presented in this chapter are similar to those used in the analysis programs [16]. These equations were selected since they permitted evaluation of all quantities

of interest after only one pass through of the data. As illustrated in Fig. 2.3, the BICEPS axis is the abscissa and the TRICEPS axis is the ordinate of the coordinate system of interest. The coordinates on the plane of the DISTILLED data for the i th window of the force level under investigation are: $(B_I(i), T_{RI}(i))$. If N is the number of data windows analyzed for a force level, the mean and standard deviation for the BICEPS dimension are:

$$M_{EANB} = \frac{1}{N} \sum_{i=1}^N B_I(i) \quad (3.2.1)$$

$$S_{DVB} = \left\{ \left[N \sum_{i=1}^N (B_I(i))^2 - \left(\sum_{i=1}^N B_I(i) \right)^2 \right] / \left[N(N-1) \right] \right\}^{1/2} \quad (3.2.2)$$

Similar relationships exist for M_{EANT} and S_{DVT} . The area of an ellipse (A_{REA}) with axes of lengths $2 S_{DVBN}$ and $2 S_{DVTN}$ is:

$$A_{REA} = \pi S_{DVBN} S_{DVTN} \quad (3.2.3)$$

Since both S_{DVBN} and S_{DVTN} are functions of the angle A_{NGL1} (refer to Fig. 2.3), the ellipse of minimum area can be determined by minimizing the product $S_{DVBN} S_{DVTN}$ as a function of A_{NGL1} . These standard deviations are calculated as follows:

$$S_{DVBN} = \left\{ \frac{\left[N \left\langle C_S^2 \sum_{i=1}^N (B_I(i))^2 + 2 C_S S_N \sum_{i=1}^N B_I(i) T_{RI}(i) \right. \right. \right.}{+ \left. \left. \left. S_N^2 \sum_{i=1}^N (T_{RI}(i))^2 \right\rangle - \left\langle C_S \sum_{i=1}^N B_I(i) + S_N \sum_{i=1}^N T_{RI}(i) \right\rangle^2 \right]}{(N(N-1))} \right\}^{\frac{1}{2}} \quad (3.2.4)$$

$$S_{DVTN} = \left\{ \frac{\left[N \left\langle C_S^2 \sum_{i=1}^N (T_{RI}(i))^2 - 2 C_S S_N \sum_{i=1}^N B_I(i) T_{RI}(i) \right. \right. \right.}{+ \left. \left. \left. S_N^2 \sum_{i=1}^N (B_I(i))^2 \right\rangle - \left\langle C_S \sum_{i=1}^N T_{RI}(i) - S_N \sum_{i=1}^N B_I(i) \right\rangle^2 \right]}{(N(N-1))} \right\}^{\frac{1}{2}} \quad (3.2.5)$$

where

$$\begin{aligned} C_S &= \cos (A_{NGL1}) \\ S_N &= \sin (A_{NGL1}) \end{aligned} \quad (3.2.6)$$

From these equations, it is clear that A_{REA} is a complex function of A_{NGL1} . For this reason, an iterative technique was used to determine A_{NGL1} such that the change in the calculated A_{REA} between successive approximations was less than 0.01% and A_{REA} was minimized.

Other quantities of interest were the slope (S_{LOP}) and the intercept with the TRICEPS axis (N_{TCPT}) of the linear least squares fit to the data.

$$S_{\text{LOP}} = \frac{\left[N \sum_{i=1}^N B_I(i) T_{RI}(i) - \sum_{i=1}^N B_I(i) \sum_{i=1}^N T_{RI}(i) \right]}{\left[N \sum_{i=1}^N (B_I(i))^2 - \left[\sum_{i=1}^N B_I(i) \right]^2 \right]} \quad (3.2.7)$$

$$N_{\text{TCPT}} = \left[\sum_{i=1}^N T_{RI}(i) - S_{\text{LOP}} \sum_{i=1}^N B_I(i) \right] / N$$

The correlation coefficient "r" was also calculated. The range of values which r assumes is: $0 \leq |r| \leq 1$. When $|r|$ approaches 1, the data has a strong linear trait.

$$r = \frac{\left[\sum_{i=1}^N B_I(i) T_{RI}(i) - M_{\text{EANB}} \sum_{i=1}^N T_{RI}(i) - M_{\text{EANT}} \sum_{i=1}^N B_I(i) + N M_{\text{EANB}} M_{\text{EANT}} \right]}{\left[(N-1) S_{\text{DVB}} S_{\text{DVT}} \right]} \quad (3.2.8)$$

Certain normalized quantities can be calculated to determine whether or not a given uni-dimensional distribution is Gaussian [17]. An estimate of the skewness, or lack of symmetry about the mean, of the distribution as measured along line L1 is A_{LPH3BN} .

$$A_{\text{LPH3BN}} = \frac{\text{Third central moment (along line L1)}}{(S_{\text{DVB}})^3} \quad (3.2.9)$$

If $A_{\text{LPH3BN}} \neq 0$, the distribution is skewed and the degree of skewness is proportional to the magnitude of A_{LPH3BN} . A similar relationship can be derived for the symmetry of the distribution measured along the other axis of the minimum area ellipse. A measure of the kurtosis (or peakedness) of

the distribution along line L1 is A_{LPH4BN} .

$$A_{LPH4BN} = \frac{\text{Fourth central moment (along line L1)}}{(S_{DVB N})^4} \quad (3.2.10)$$

For a normal distribution, $A_{LPH4BN} = 3$. If $A_{LPH4BN} > 3$, the distribution is somewhat more peaked than the Gaussian distribution. A similar relationship can be derived to measure the kurtosis of the distribution along the ellipse's other axis. The expanded forms of the equations for A_{LPH3BN} and A_{LPH4BN} can be found in many texts [17].

3.3 Determination of the Percentage of Data Points within an Ellipse

Once the coordinates of the foci of an ellipse are known a simple test may be used to determine if some point "P" having coordinates $(B_I(i), T_{RI}(i))$ lies on or within it. The two foci, " F_1 " and " F_2 ", are located on the ellipse's major axis. (Refer to Fig. 2.3.) The point P lies on or within the ellipse if the following condition holds:

$$L_1 + L_2 \leq 2A \quad (3.3.1)$$

where A is one-half of the length of the major axis of the ellipse (For Fig. 2.3, $A = S_{DVTN}$), L_1 is the distance from P to F_1 and L_2 is the distance from P to F_2 .

If the coordinates of F_1 are (F_{1BI}, F_{1TRI}) and those of F_2 are (F_{2BI}, F_{2TRI}) , L_1 and L_2 may be evaluated with the aid of the Pythagorean theorem:

$$L_1 = [B_I(i) - F_{1BI})^2 + (T_{RI}(i) - F_{1TRI})^2]^{1/2} \quad (3.3.2)$$

$$L_2 = [(B_I(i) - F_{2BI})^2 + (T_{RI}(i) - F_{2TRI})^2]^{1/2}$$

The coordinates of the foci of an ellipse may be calculated by using the following relationships:

$$F_{1BI} = M_{EANB} + F \cos(\theta_1)$$

$$F_{2BI} = M_{EANB} - F \cos(\theta_1) \quad (3.3.3)$$

$$F_{1TRI} = M_{EANT} + F \sin(\theta_1)$$

$$F_{2TRI} = M_{EANT} - F \sin(\theta_1)$$

where F is the distance between either of the foci and the bidimensional mean so that:

$$F = [A^2 + B^2]^{1/2} \quad (3.3.4)$$

where B is the length of the minor axis of the ellipse (For Fig. 2.3, $B = S_{DVBN}$) and, where θ_1 is equal to A_{NGL1} if $S_{DVBN} \geq S_{DVTN}$ or it is equal to $A_{NGL1} + \frac{\pi}{4}$ if $S_{DVBN} < S_{DVTN}$. Once it is possible to determine if a particular data point "P" lies within a certain ellipse, the calculation of the percentage of data points lying within the ellipse is straightforward. As mentioned in Chapter 2, it is useful to allow the isoprobability ellipses to enlarge so as to increase the percentage of data points lying within them. An ellipse enlarged by a factor " P_{UFF} " will have axes lengths of $P_{UFF} S_{DVBN}$ and $P_{UFF} S_{DVTN}$. By expressing A and B in the previous equations in terms of $P_{UFF} S_{DVBN}$ and $P_{UFF} S_{DVTN}$, a more suitable form of the equation is obtained.

As ellipses enlarge, they overlap. Since it is

desired to retain only distinct or non-overlapping regions, one ellipse of each pair of overlapping ellipses must be discarded. Therefore, it is necessary to determine when two ellipses overlap.

Consider ellipses J and I, each enlarged by a factor P_{UFF} . Coordinates of the points lying on ellipse I will have the following range of values when the ellipse's axes are used as the coordinate system:

$$\begin{aligned} 0 &\leq |V_{XN}| \leq A \\ 0 &\leq |V_{YN}| \leq B \end{aligned} \quad (3.3.5)$$

where V_{XN} is the coordinate measured along the abscissa (the ellipse's major axis) and V_{YN} is the coordinate as measured along the ordinate (the ellipse's minor axis).

By choosing a value for V_{XN} which lies within the appropriate limits, the two values of V_{YN} are determined as:

$$V_{YN} = \pm B \{ | \langle 1.0 - V_{XN}^2/A^2 \rangle | \}^{1/2} \quad (3.3.6)$$

The two points on the ellipse in this coordinate system are (V_{XN}, V_{YN}) and $(V_{XN}, -V_{YN})$. To determine the coordinates of these points in the BICEPS-TRICEPS plane the following transformations are used:

$$\begin{aligned} B_I(1) &= V_{XN} \sin(\theta_2) + V_{YN} \cos(\theta_2) + M_{EANB} \\ T_{RI}(1) &= V_{YN} \sin(\theta_2) - V_{XN} \cos(\theta_2) + M_{EANT} \\ B_I(2) &= V_{XN} \sin(\theta_2) - V_{YN} \cos(\theta_2) + M_{EANB} \\ T_{RI}(2) &= -V_{YN} \sin(\theta_2) - V_{XN} \cos(\theta_2) + M_{EANT} \end{aligned} \quad (3.3.7)$$

where θ_2 is equal to $A_{\text{NGL1}} + \frac{\pi}{4}$ if $S_{\text{DVBN}} \geq S_{\text{DVTN}}$ or it is equal to 0 if $S_{\text{DVTN}} > S_{\text{DVBN}}$ and where the transformed coordinates of the point $(V_{\text{XN}}, V_{\text{YN}})$ are $(B_{\text{I}}(1), T_{\text{RI}}(1))$ while those of point $(V_{\text{XN}}, -V_{\text{YN}})$ are $(B_{\text{I}}(2), T_{\text{RI}}(2))$.

Now that the coordinates of the points on ellipse I are known, equations (3.3.3) may be used to find the foci of ellipse J. To determine whether or not the point $(B_{\text{I}}(1), T_{\text{RI}}(1))$ or $(B_{\text{I}}(2), T_{\text{RI}}(2))$ lies within ellipse J, condition (3.3.1) is used.

In practice, it has been found that if sixty-four points are used to approximate the Ith ellipse, it is possible to determine the P_{UFF} factor at which two ellipses first overlap to within a resolution of ± 0.05 . Since it was observed that the percentage of data points within an ellipse is not a rapidly varying function of P_{UFF} for the values of interest, this resolution was considered to be sufficient. In circumstances where S_{DVBN} and S_{DVTN} differ by many orders of magnitude (this occurs only for power law detectors of high power) it is necessary to use double precision throughout these calculations.

3.4 Discarding Ellipses

It is necessary to discard one ellipse of a pair overlapping at a particular P_{UFF} value. Two conditions must be met when discarding ellipses:

- (i) The ellipse corresponding to the force level of the resting arm may not be discarded as it is essential in

any practical situation.

- (ii) Of all the possible sets of ellipses which may be discarded to eliminate overlap, the one discarding the fewest ellipses is to be chosen as it maximizes the number of distinct levels.

The first condition is easily met. It demands that any ellipse overlapping the ellipse representing the resting state, is always discarded. The second condition can be expressed in mathematical form.

Consider that at some value of P_{UFF} , the number of ellipse pairs which have overlapped is "n". These ellipses are each denoted by a "level number" between 1 and K, where K is the total number of force levels considered. Let the level numbers of the elements of the ℓ th pair of overlapping ellipses be $K_{FP}(\ell)$ and $K_{SP}(\ell)$. The n conditions which must be met to avoid overlapping are:

$$\text{(Either } K_{FP}(\ell) \text{ or } K_{SP}(\ell) \text{ be discarded*)} \quad \ell=1 \text{ to } n \quad (3.4.1)$$

*If $K_{FP}(\ell)$ or $K_{SP}(\ell)$ is the force level for which the arm lies resting then the other level of the pair is discarded. Utilizing Boolean notation, these n conditions may be expressed as one:

$$\text{Discard } (K_{FP}(1) + K_{SP}(1)) \cdot (K_{FP}(2) + K_{SP}(2)) \cdot \dots \cdot (K_{FP}(n-1) + K_{SP}(n-1)) \cdot (K_{FP}(n) + K_{SP}(n)) \quad (3.4.2)$$

This condition may be written in the form:

$$\begin{aligned} &\text{Discard } (K_{FP}(1) \cdot K_{FP}(2) \cdot \dots \cdot K_{FP}(n-1) \cdot K_{FP}(n)) \\ &+ (K_{FP}(1) \cdot K_{SP}(2) \cdot \dots \cdot K_{FP}(n-1) \cdot K_{FP}(n)) \dots \\ &+ (K_{SP}(1) \cdot K_{SP}(2) \cdot \dots \cdot K_{SP}(n-1) \cdot K_{SP}(n)) \quad (3.4.3) \end{aligned}$$

To satisfy this condition, it is necessary to discard any one of the set of logically anded elements. If the m th such group of elements is denoted as $P(m)$ then (3.4.3) becomes:

$$\text{Discard } P(1) \text{ or } P(2) \text{ or } \dots \text{ or } P(m) \text{ or } \dots \text{ or } P(j) \quad (3.4.4)$$

where, clearly, $j = 2^m$. Although 2^m products exist, many of them are identical. It is also not true that each product must contain m unique elements, since a particular ellipse may occur in more than one of the m pairs.

Therefore the problem involves the selection of a product $P(m)$ which is one of the group of unique products having the minimum number of unique elements. This logically simple process is practically impossible to perform without the aid of a digital computer when K is large (K was typically 23 in our experiments) and when m is large (common values of m were in the range of 30 to 50, i.e. 30 to 50 pairs of overlapping ellipses).

CHAPTER 4

MEASUREMENT AND ANALYSIS TECHNIQUES

This chapter will review the design considerations and describe the necessary hardware and software as well as the repertoire of experiments performed in this study. An overall view of the data acquisition, storage, analysis and display system is presented in Fig. 4.3. Further detailed information regarding the hardware and software can be found in a technical report of this work [16].

4.1 Data Acquisition

4.1.1 Electrodes and Amplifiers for the EMG:

To obtain high quality, reproducible results, care must be taken with signal measurement and amplification. The type of electrodes and the nature of the experiment determine the appropriate amplifiers. Dry surface electrodes were chosen since they require less preparation and cause less skin irritation than wet surface electrodes. Coin silver electrodes of diameter 1.7 cm. were constructed by grinding one face of a pre-1967, silver Canadian dime to a smooth surface. A lead was soldered to the other side for electrical contact. Electrode preparation prior to experimentation involved

cleaning the ground surface with a fine emery paper. A similar arrangement was used by Geddes et al (18) who determined that the resistive components of such electrodes (R) vary with time (t) in the following fashion:

$$R = 1284 e^{-0.34t} \text{ K}\Omega + 66.3 \text{ K}\Omega \quad (4.1.1)$$

where t is time in minutes and t=0 corresponds to the time of application of the electrodes to the skin.

As can be seen from examining (4.1.1), $R = 1.3 \text{ M}\Omega$ at t=0 and it decreases until, at $t \approx 25 \text{ min.}$, $R \approx 66 \text{ K}\Omega$. Such a great variation in electrode impedance will cause a varying proportion of the signal to appear as a potential across the amplifier's input impedance (z_i). This produces the same effect as if R was constant but the amplifier's gain increased with time. If z_i is sufficiently large, these changes due to R are negligible. A centre to centre inter-electrode spacing of 2.2 cm was chosen since it permitted convenient mounting of the electrodes on a foam pad beneath the epoxy encapsulated amplifier (see Fig. 4.1(a)).

A study of the power spectral density (p.s.d.) in the muscles of the hand, using bi-polar surface electrodes, revealed that significant spectral power existed only in the 10-250 Hz band of frequencies. Using similar electrodes to the ones which we used, but with an inter-electrode spacing of 3.3 cm, de Bruin (4) observed that the p.s.d. outside the band of 10-100 Hz was less than 15% of the maximum. The maximum was located at approximately 50 Hz. For frequencies greater than 250 Hz, the p.s.d. was less than 2% of the

maximum and it diminished rapidly with frequency.

The presence of high value (200 mv. P-P) line frequency potentials in a human subject who is not extremely well grounded imposes difficulties. On certain occasions, these potentials were more than three orders of magnitude greater than the signals of interest. Such noise could be eliminated by filtering but this would cause considerable signal distortion since the peak in the EMG p.s.d. is at 50 Hz. The traditional solution, and the one used in the previously mentioned p.s.d. studies, is to rely on the common mode rejection of a differential amplifier to reduce line frequency noise as it is primarily common mode.

If the amplifier is remotely connected to the electrodes by a standard coaxial cable, considerable potentials of a wide bandwidth can be generated by cable motion. To reduce this problem, a specially designed cable may be used [21] or the amplifier may be located in close proximity to the electrodes [20].

Considering the above information, an amplifier circuit, based on a commercially available integrated circuit, was designed and tested. It produced low-noise high quality EMG's. The specifications of this amplifier are given in TABLE 4.1. Fig. 4.1(a) is a view of this epoxy encapsulated amplifier showing the electrodes mounted on foam pads attached to the encapsulation. A third electrode, used as ground, is also shown mounted on its own foam padded holder. The use of a dry surface electrode as a ground provides good isolation

Active element used for instrumentation amplifier:
 ADS21KD instrumentation Amplifier, Analog Devices Corp.
 (dual-in-line ceramic package)

Specifications for Instrumentation Amplifier

Gain:	60 dB
3 dB Bandwidth:	10 Hz to in excess of 20 KHz
CMRR, 10 to 250 Hz:	110 dB min.
Input Bias Current: (either input)	40 nA max.
Differential Input Impedance (z_i):	$3 \times 10^9 \Omega$
Common Mode Input Impedance:	$6 \times 10^{10} \Omega$
Power Supply:	± 9 V (transistor batteries)
Encapsulation:	Casting resin. Electrodes mounted on foam pad beneath encapsulation. Dimensions of encapsulated amplifier with electrode pads: 4 x 6 x 3.5 cm.

Specifications of Instrumentation Amplifier
 followed by Gain Augmenting Amplifier

Gain:	Selectable: 60-80 dB
3 dB bandwidth:	10-1000 Hz
RMS noise measured by monitoring the inactive* biceps muscle (referred to input):	11 μ V
* This includes noise due to residual EMG activity and other physiological sources such as the EKG	

Table 4.1 Amplifier Specifications

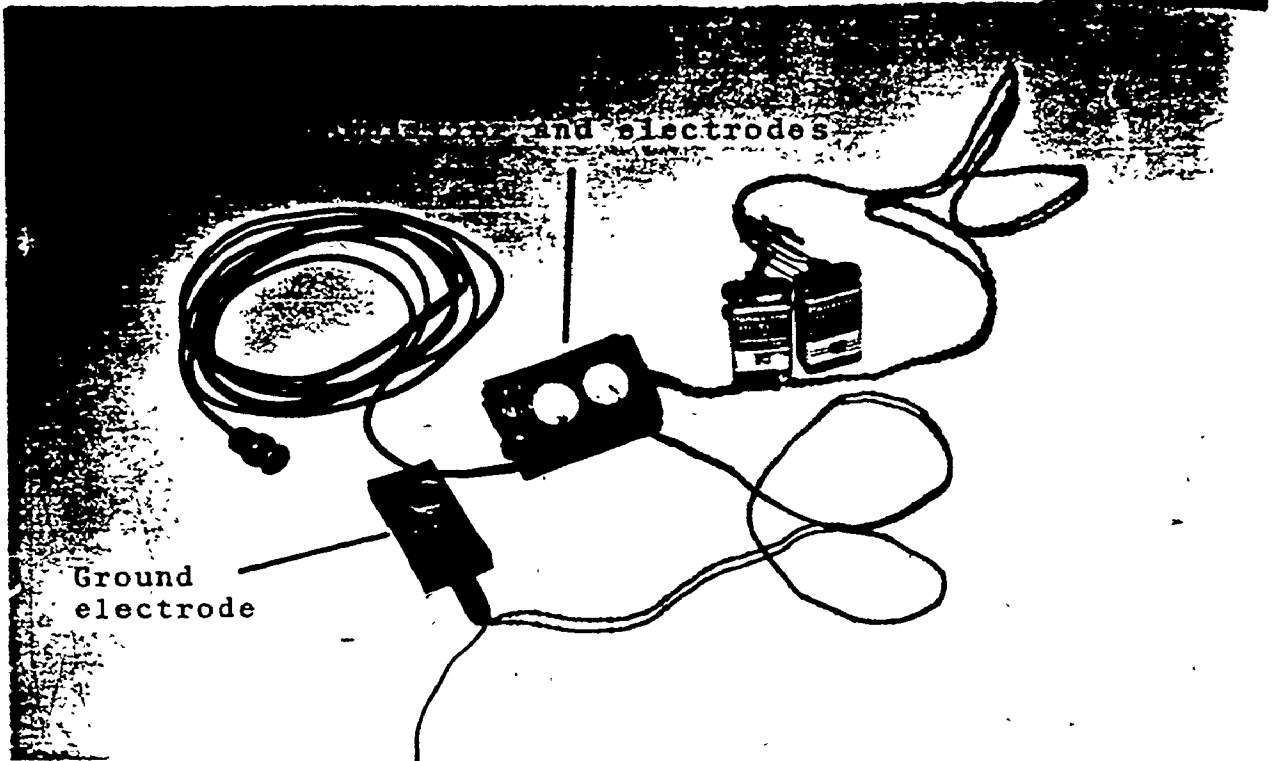


Fig. 4.1(a) Epoxy Encapsulated Amplifier and the Surface Electrodes

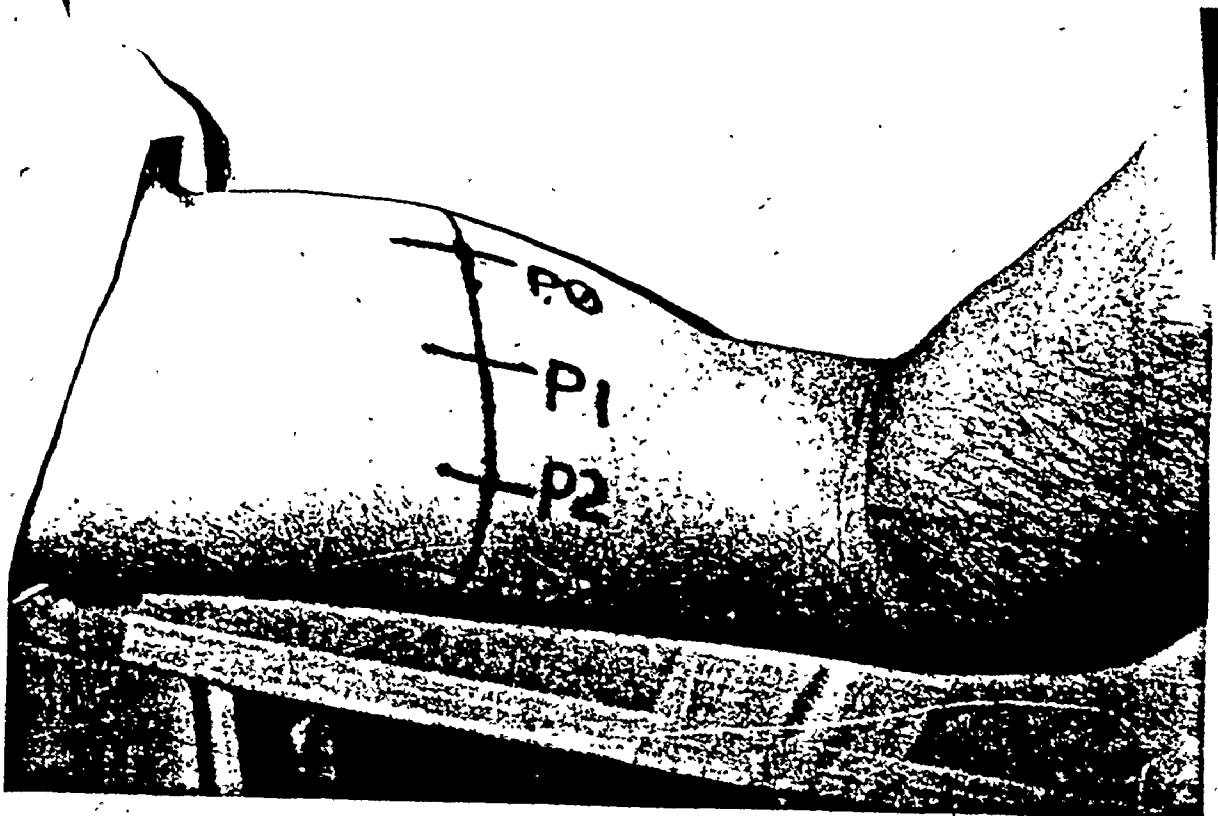


Fig. 4.1(b) Electrode positions. (lateral view of right arm)

of the subject from power line ground (66 K Ω). It also prevents damage to the amplifier's input terminals from large static potentials which may exist in an ungrounded subject. To achieve such a high z_i , it was necessary to D.C. couple the electrodes to the amplifier. This is undesirable since it requires that a continuous current pass through the electrodes to satisfy the amplifier's input bias requirements. However, for our amplifier, bias currents were so low (40 nA max.) that this was not considered a problem.

4.1.2 Positioning of Electrodes on the Upper Arm:

As previously discussed, some variation in results is expected as a function of electrode placement. The effect of electrode position on the quality of the results was examined at a total of four different positions for the flexor signal and at one position for the extensor signal. This procedure was adopted since preliminary results were inferior when the flexors were primarily active as compared to the case where the extensors were the protagonists. Furthermore, a marked variation in the quality of results for the flexors was observed with electrode placement.

The electrodes used to monitor the extensor signal were placed over the crest of the triceps muscle. Electrode position P_0 for the flexor signal was chosen as the crest of the biceps muscle while the three other positions (P_1, P_2, P_3) were centred along the horizontal line joining P_0 with the electrode position for the extensor (P_E) and located on the

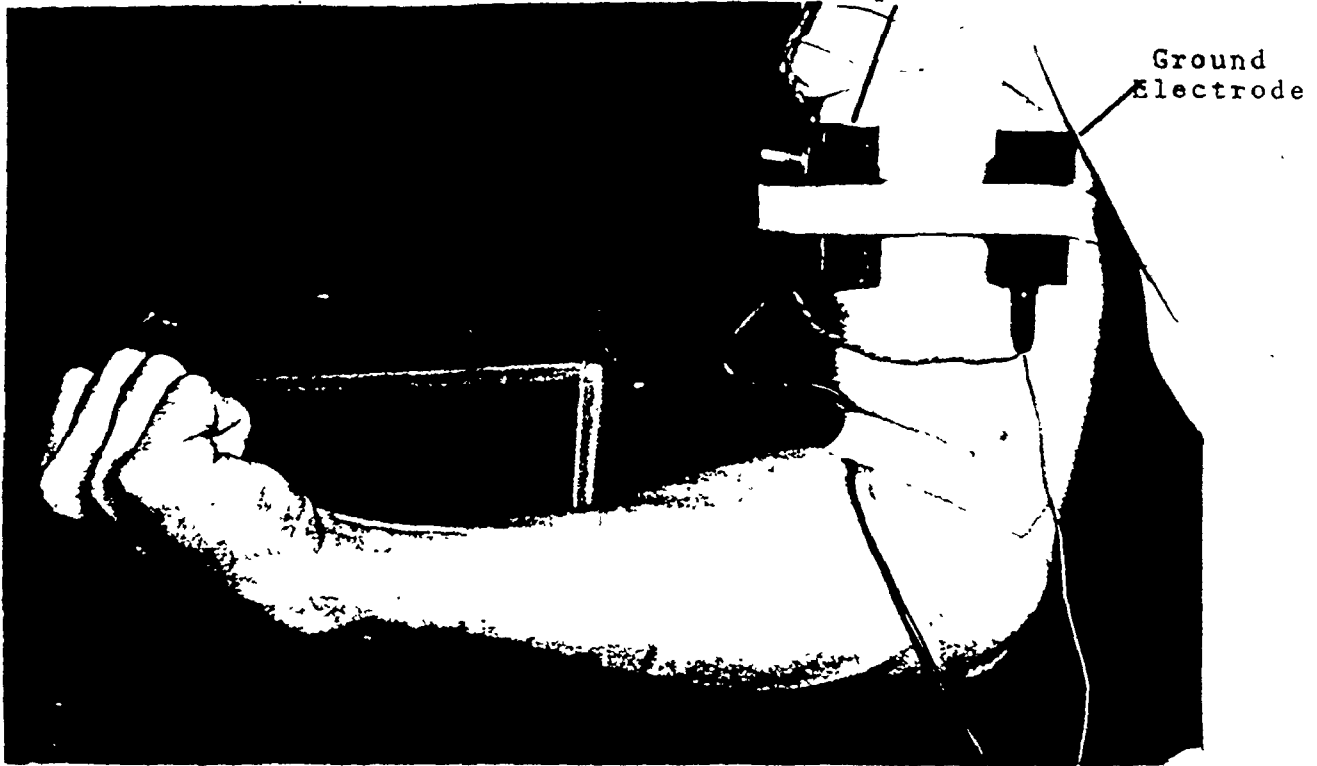


Fig. 4.1(c) Positioning of the Flexor EMG Amplifier and the Ground Electrode (Medial view of right arm)

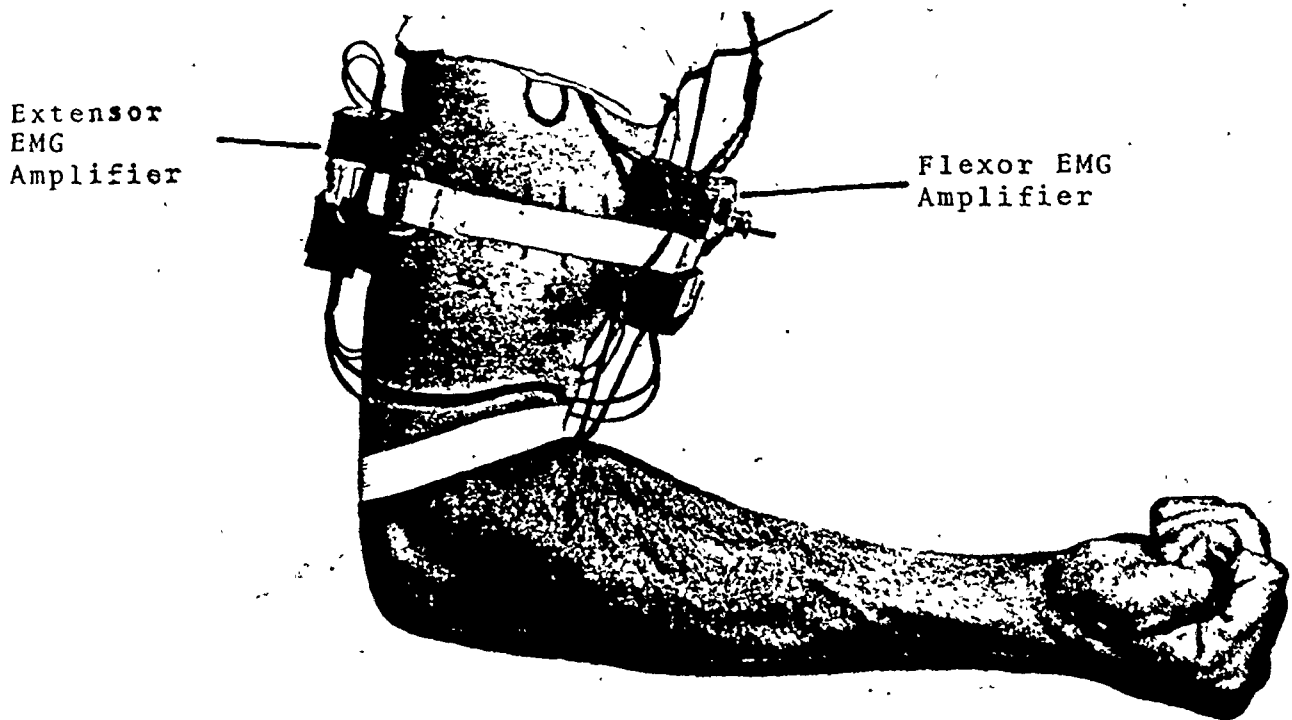


Fig. 4.1(d) Positioning of both EMG amplifiers (Lateral view of right arm)

lateral aspect of the arm. P_1 , P_2 and P_3 were located at $1/6$, $1/3$, and $1/2$ of the distance from P_0 to P_E , away from P_0 , respectively. Fig. 4.1(b) shows the actual electrode positions. Fig. 4.1(c) illustrates the positioning of the flexor amplifier and the ground electrode on the arm. The ground electrode is located on the line segment joining P_0 and P_E located on the medial aspect of the arm. Since this location is not over any large muscles, it should provide a good reference. It is not strictly required that the reference electrode be at an inactive site because the amplifiers employed have a high CMRR. A lateral view of the upper arm showing both instrumentation amplifiers in position is given in Fig. 4.1(d).

4.1.3 The Force Transducer:

An inexpensive force transducer was designed and constructed using strain gauges in a balanced bridge configuration. The strain gauges were mounted on a flexible steel bar which was clamped at one end but free to move at the other (Fig. 4.2(a)). A force exerted at the free end causes an elastic deformation of the beam producing a change in the strain gauge's resistance which results in an imbalance of the bridge. With the appropriate electronics, this imbalance may be measured. The properties of the force transducer so constructed are presented in TABLE 4.2.

During experimentation, the arm is positioned as shown in Fig. 4.2(b). The elbow is resting on a padded shelf. The wrist is in a collar which is used to exert a force, during isometric contraction, against the resistance

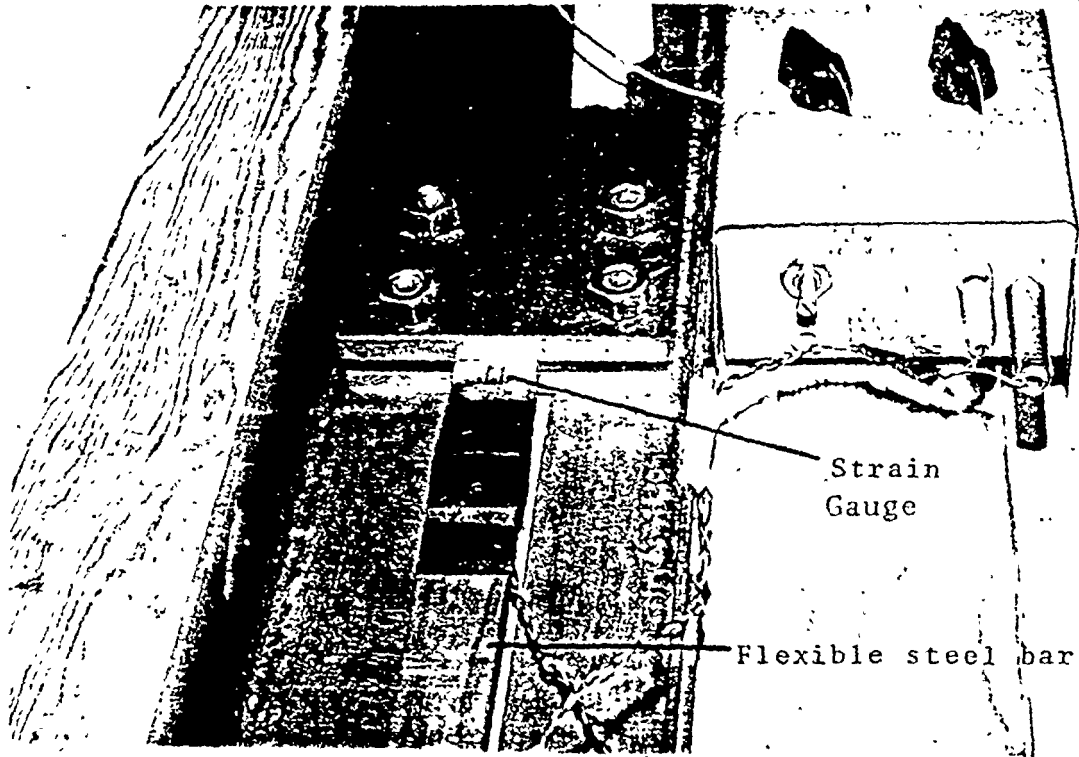


Fig. 4.2(a) Force Transducer

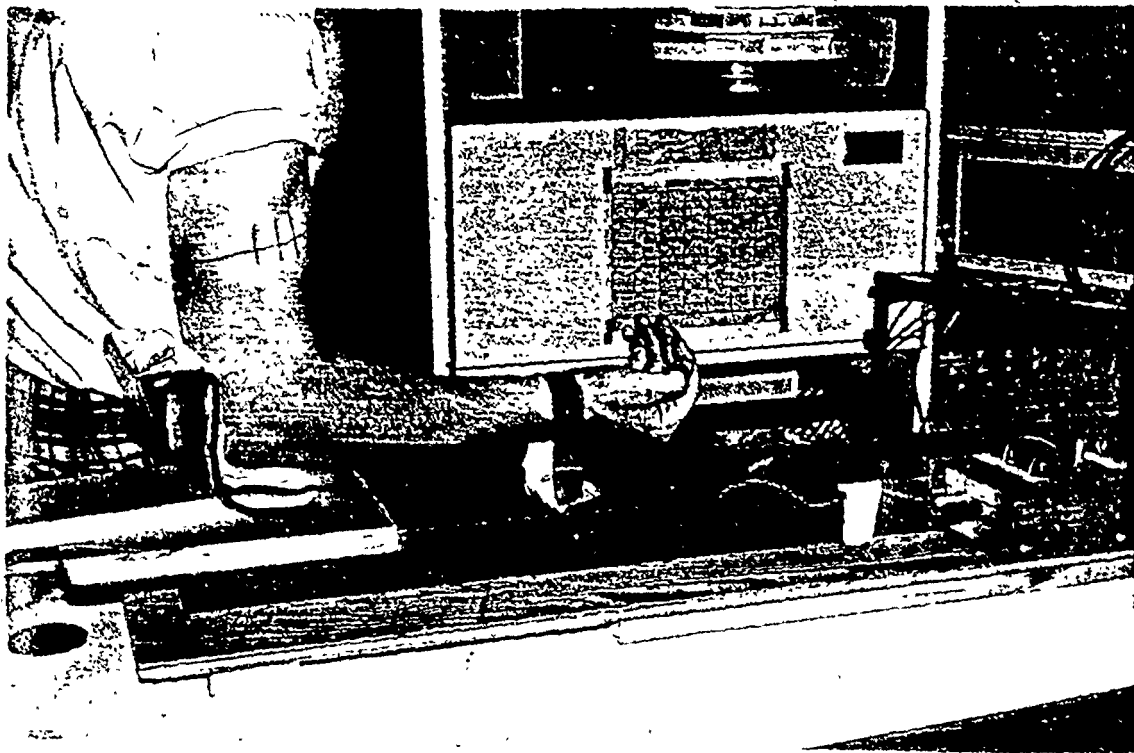


Fig. 4.2(b) Position of Arm During Experimentation

RANGE OF MEASUREMENT:	-7.8 Kg. to +11.0 Kg.
OUTPUT VOLTAGE:	$V_{OUT} = 0.5 (F_r) + V_{OFF}$
	where: F_r is the net force in Kg. exerted on the beam at the point of measurement
	: V_{OFF} is an adjustable offset voltage
SENSITIVITY:	$\frac{\text{Change in } V_{OUT}}{\text{Change in } F_r} = 0.5 \text{ V/Kg.}$
MAXIMUM UNCERTAINTY*:	$\pm 6\%$ where: $0 \leq F_r \leq 0.5 \text{ Kg.}$ $\pm 3\%$ where: $1.0 \text{ Kg.} \leq F_r $

* This includes error due to calibratability, linearity, long term drift and short term drift due to metal creep.

Table 4.2 Properties of Force Transducer

of the force transducer. The elbow joint angle is maintained roughly at ninety degrees by using the right angle of the elbow rest as a reference. As different forces are exerted, the bar bends and it is necessary to adjust the vertical position of the elbow pad to maintain the desired elbow angle. If adjustments are made so that for a particular measurement:

$$V_{OFF} = -0.5 F_D \text{ volts} \quad (4.2.1)$$

where F_D is the desired force in Kg., then V_{OUT} will be zero volts when that particular force is exerted. This permits the use of an oscilloscope on a high sensitivity setting (20 mv./cm. i.e. 40 mg./cm.) to provide visual feedback to the subject, thereby achieving the desired degree of controllability. Using this method, the subject was able to maintain such a constant force that the standard deviations were 1-2% of the means throughout the force range of measurement.

In a typical experiment, a total of 23 different force levels were used. It was necessary to take the weight (W) of the resting forearm, as measured at the wrist, into account. These twenty-three force levels are presented in TABLE 4.3 with associated force level numbers. At any level, the contribution to the measured force by the muscles of the upper arm is simply the total force measured plus W . Force level #11, for which the net force is $-W$, is the resting position. When the net force is 0.0 Kg., the weight of the forearm is supported by the flexors.

For very high force levels, 2.0 Kg. increments in force were used between levels; while 1.0 Kg. increments were

FORCE LEVEL NUMBER	FORCE (Kg.)
1	$-(7+W^*)$
2	$-(6+W)$
3	$-(5+W)$
4	$-(4+W)$
5	$-(3+W)$
6	$-(2.5+W)$
7	$-(2.0+W)$
8	$-(1.5+W)$
9	$-(1.0+W)$
10	$-(0.5+W)$
11	$-W$
12	0
13	0.5
14	1
15	1.5
16	2
17	2.5
18	3
19	4
20	5
21	6
22	8
23	10

* W represents the weight of the resting forearm as measured at the wrist

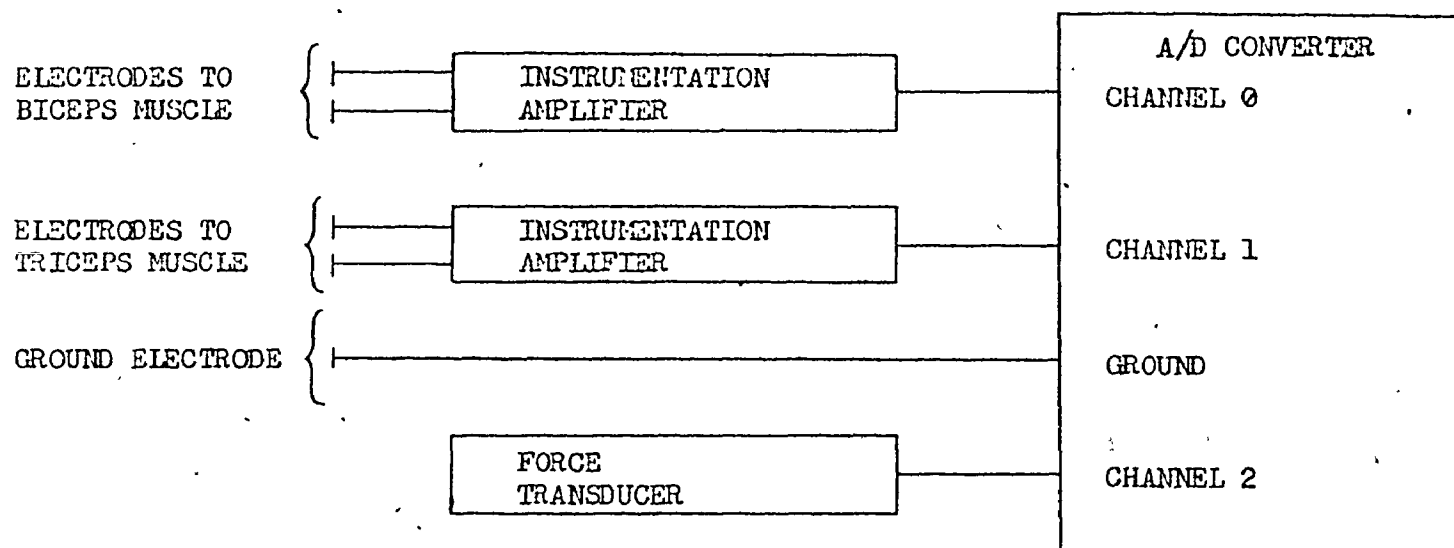
Table 4.3 Force Levels

employed at moderate force levels and 0.5 Kg. increments at low force levels. These increments were chosen since fine control of force in absolute units is possible only at lower forces where many distinct regions can be defined. Larger increments are necessary at higher force levels because, although the percentage controllability remains roughly constant, the absolute controllability of force by the subject diminishes. The use of low force levels for prosthetic control is desirable since prolonged effort at high forces may cause fatigue, and EMG properties have been observed to alter in the fatigued muscle (19).

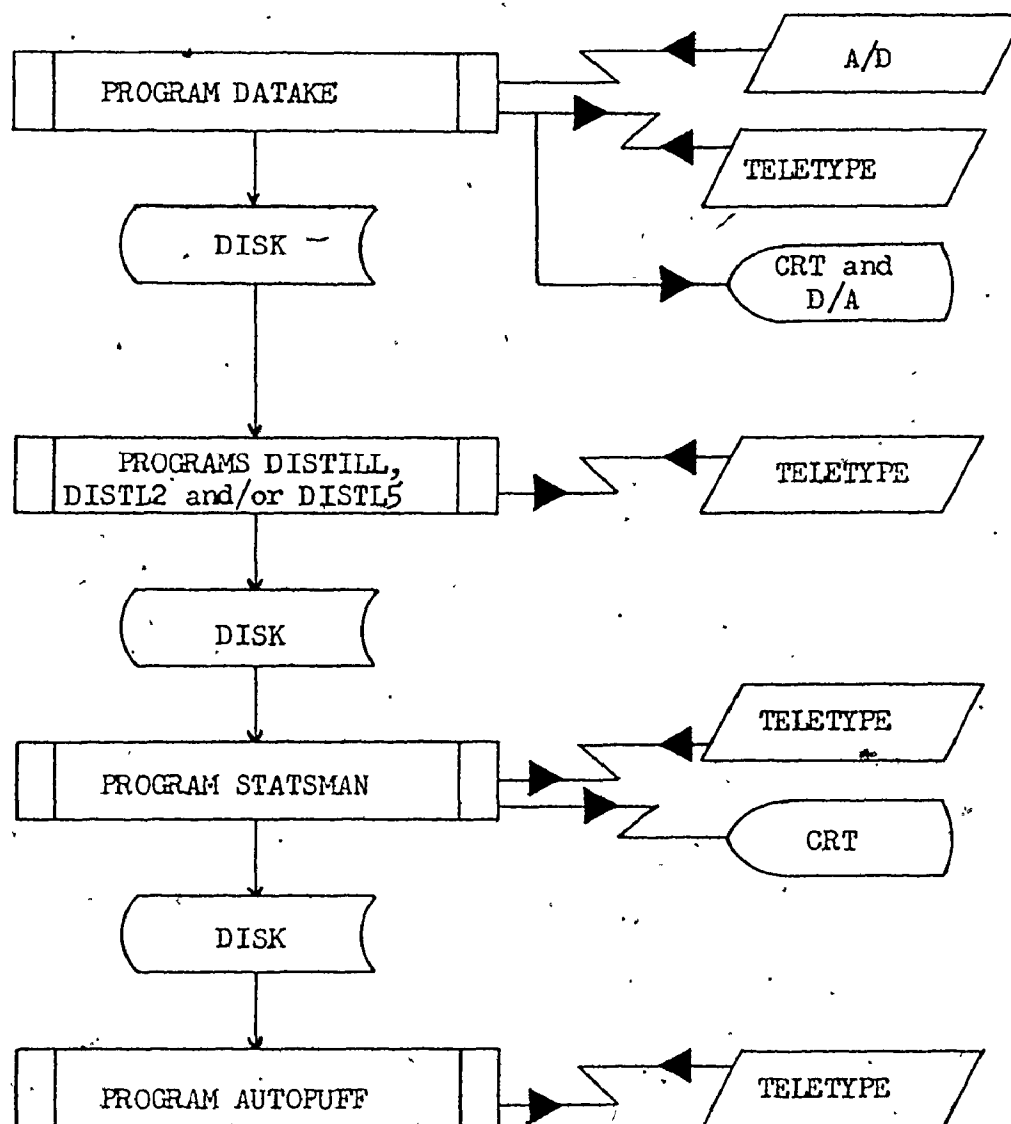
4.1.4 Sampling and Storing of Signals :

The overall scheme of signal acquisition is shown in Fig. 4.3. The two EMG signals and the signals from the force transducer are applied to an eight channel 12-bit A/D unit of the NOVA 830 minicomputer. This unit has a dynamic range of ± 5.0 volts. A flow diagram illustrating the software used in data acquisition and analysis is presented in Fig. 4.3(b).

Program DATAKE is an interactive program which communicates with the user via the teletype (TTY), CRT (Tektronics 4010 terminal), and D/A units. It accepts program control commands from the user over the teletype. With DATAKE, it is possible to acquire, store and examine (utilizing the 4-channel D/A unit) data sampled over a ten second sampling interval on three A/D channels. All data collected during a ten



(a)



(b)

Figure 4.3 Data acquisition, storage, analysis and display system.

second interval is stored in core buffers and may be transferred to disk files for permanent storage.

From the previously mentioned measurements of the EMG's p.s.d., it is clear that the maximum frequency of interest is 250 Hz. In the present measurement system, even though noise frequencies extended beyond 250 Hz., the R.M.S. noise was so small compared with the EMG signals of interest that aliasing of this noise with the signal was not important. For this reason a 500 Hz sampling rate was considered sufficient.

In a preliminary study it was observed that, although a small change occurred in the magnitude of values as sampling rate decreased from 1000 to 500 Hz for the biceps EMG, no appreciable deterioration in the SNR or in the sensitivity of the processed values to the force level, occurred. Rather than restructure the programs utilized in this early study, a sampling rate of 1000 Hz was retained for the flexor signal while one of 500 Hz was used for the extensors.

From Neilson's measurements [6], it is clear that a sampling rate of 20 Hz is sufficient for monitoring the force signal in this situation where central nervous system voluntary control is used. It may also be true that some of the reflex neural network is used in maintaining the desired constant force over a ten second sampling window. Measurements concerning such reflex systems [22] have been performed and it is observed that frequencies in excess of 10 Hz are

present. During experimentation, it was possible to obtain an estimate of the frequencies involved in force control by observing the time course of force fluctuations using a storage oscilloscope. From this, it was observed that all frequencies in excess of 4Hz have amplitudes of less than ± 10 mg. This is insignificant when compared to the forces of interest.

A typical experiment consisted of twenty-three different force levels as described in Section 4.1.3. The number of ten second data sampling sequences, or records, which were taken per experiment was determined by the disk space available. Each record required 60 disk blocks for storage (one block is 256 words). A 1.25 mega-word capacity, disk pack was utilized. The present experiments involved 48 records; two being taken at each of the twenty-three force levels and an additional two taken with the muscle as inactive as possible. Inactivity was achieved by allowing the arm to hang loosely from the shoulder in a relaxed fashion (23). The two records of the inactive muscle were used to estimate the measurement noise.

4.2 Computer Realization of the Various Signal Processors

The data stored on disk is analyzed by the various signal processing methods using data windows of filter time constants of 0.5 seconds. The analysis is performed by one or more of the following programs: DISTILL, DISTL2 and DISTL5. TABLE 3.1 indicates the signal processing techniques employed by each of these programs. The data acquisition system's gain is taken into account so that all EMG data is scaled in millivolts referred to the electrode.

These programs are interactive. It is necessary to input the number of records to be analyzed (typically 48) and the desired force at each record. To reproduce the actual net force, the desired force is added to the deviations from the desired force which were sampled and stored.

From these values, the mean and the standard deviation of the force are found and tabulated by DISTILL and DISTIL2.

The noise thresholds (F_{NOISE}) for use with the peak detector are calculated from one of the noise records of the EMG from each muscle. F_{NOISE} is evaluated as that voltage which is two standard deviations in excess of the mean P-P amplitude. These programs utilize either the calculated F_{NOISE} or values of F_{NOISE} entered by the user. In this way, values averaged over many experiments for F_{NOISE} can be entered.

As depicted in Fig. 4.3, the results of these analyses are stored in disk files. This processed data is referred to as DISTILLED data.

4.3 Evaluation of Statistical Quantities

The many bivariate statistical quantities used to describe the DISTILLED data as discussed in Chapters 2 and 3 are evaluated by program STATSMAN for each of the processing methods. STATSMAN is highly interactive. It may be used to plot ellipses for the various force levels enlarged by a factor P_{UFF} , to plot DISTILLED data separately or superimposed

over the plotted ellipses, to determine the P_{UFF} factor necessary for any pair of ellipses to first touch (where $0.2 \leq P_{UFF} \leq 3.2$) and to calculate the percentage of DISTILLED data points lying within the enlarged ellipse associated with the same force level as well as the average and minimum of these percentages over several levels. The output format of the statistical results can also be chosen.

If desired, the DISTILLED data and/or the evaluated statistical parameters can be restored on disk files, each capable of accumulating data for up to eleven similar experiments. STATSMAN utilizes this accumulated data to produce the overall statistical parameters. When the total data of eleven experiments is analyzed as a unit, results for each force level are based on 220 seconds of data sampling.

It is possible that the average force over some windows will differ greatly from the mean force over the entire level. Therefore it was decided to discard all data for windows having an average which was not within $\pm 5\%$ of the mean for the particular level. In the case where data from many experiments is combined for analysis, the mean force for a level is evaluated over all of the records corresponding to the particular force level under study. No data is rejected for the force level in which the arm is resting or in which the weight of the arm is supported by the flexors since, in these cases, no feedback of the net force to the subject is used. As will soon be discussed, this rejection of certain data is performed throughout all aspects of programs STATSMAN

and AUTOPUFF.

If STATSMAN has difficulty in determining the ellipse of minimum area as outlined in Section 3.2, this indicates that poor convergence has occurred and the percentage change in area between the last successive iterations is presented. If this percentage is less than 0.5%, it is considered that the convergence is adequate.

Under certain circumstances, the round-off error in calculations will render them inaccurate. By utilizing double precision, approximately sixteen significant decimal digits are carried. If the standard deviations differ by more than six orders of magnitude, STATSMAN will print a warning message indicating poor accuracy could occur. This did not happen in any of the experiments which we performed.

A photograph of the plot produced by STATSMAN on the CRT of DISTILLED data for the SUM processor for several force levels is presented in Fig. 4.4(a). In Fig. 4.4(b), the same data is plotted but with the ellipses of minimum area superimposed. The major axes of the ellipses are shown. Since the scaling of the BICEPS and TRICEPS axes in the plot are not equal, the ellipses are somewhat distorted. The axes and axes graduations were drawn by a graphics package but all titles were dubbed.

As discussed earlier, both 0.5 and 1.0 second data windows are considered. The 1.0 second data windows are produced by combining the DISTILLED data for two consecutive 0.5 second windows and averaging. These 1.0 second windows

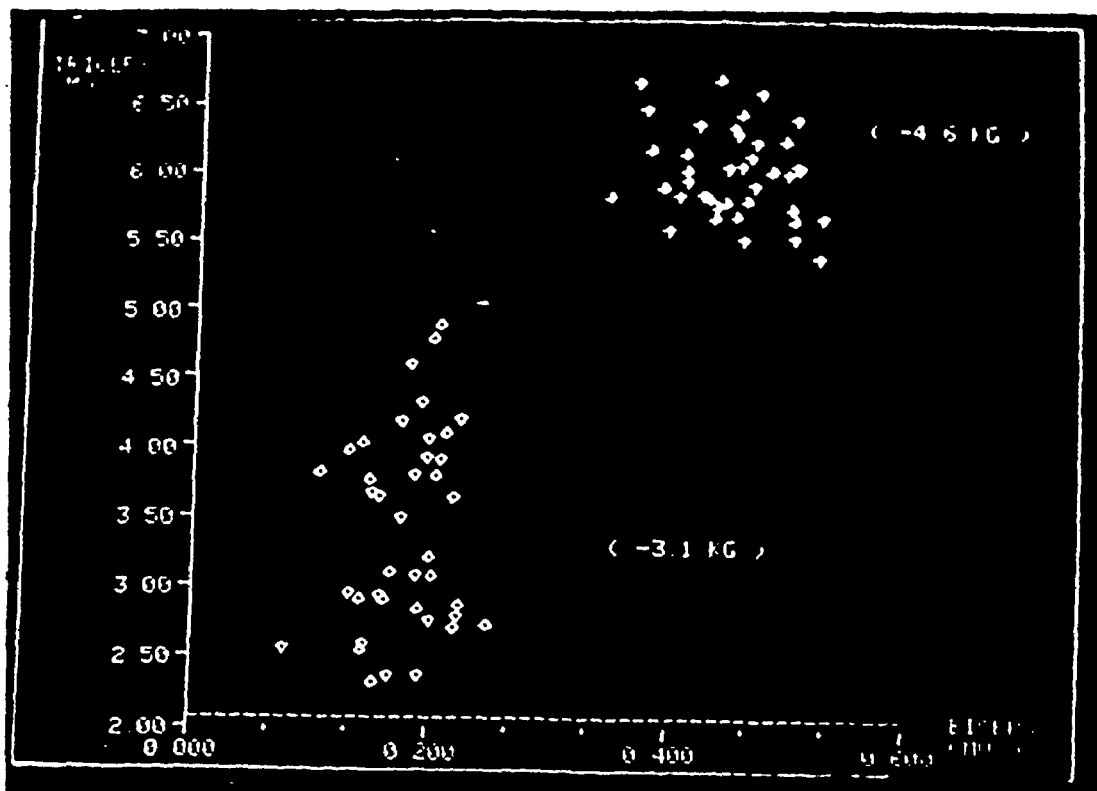


Fig. 4.4(a) Plot of DISTILLED Data for SUM processor

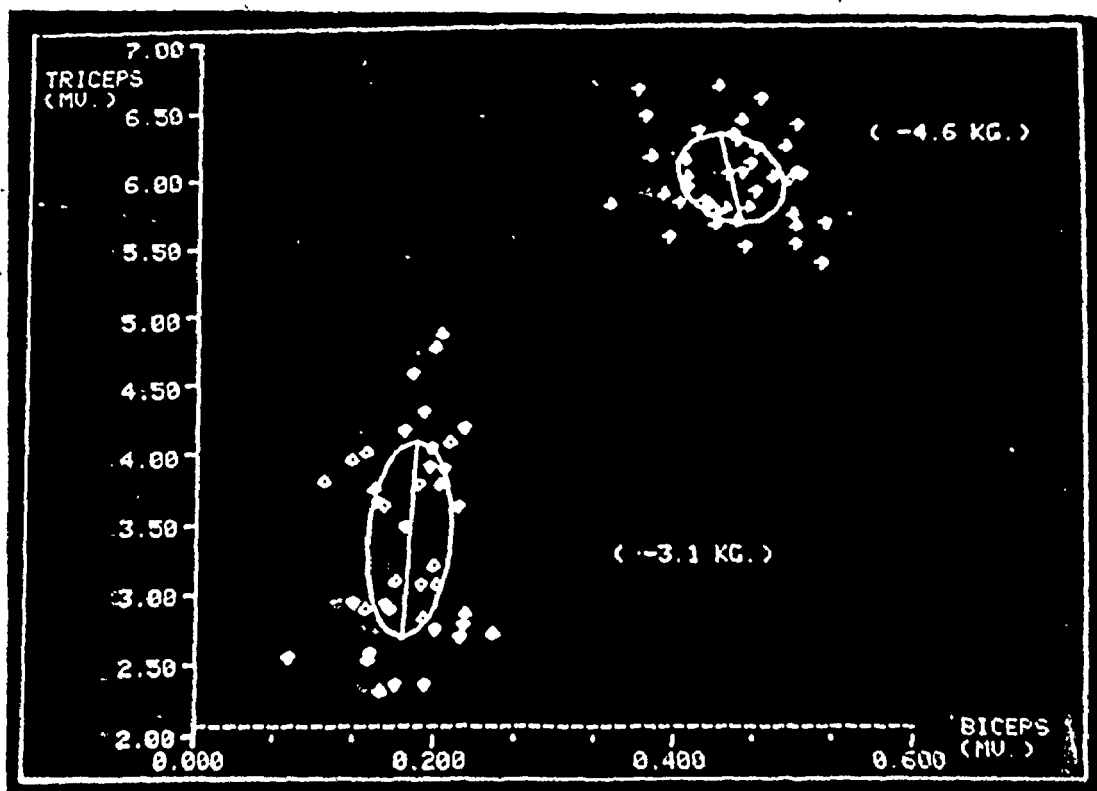


Fig. 4.4(b) Plot of Ellipses for SUM processor

slide by 0.5 seconds so that consecutive windows overlap and nineteen windows per record are possible. One shortcoming of STATSMAN and AUTOPUFF is that averaging to obtain values for a 1.0 second window is applied, regardless of method. When considering methods which evaluate a running sum, it is more consistent to simply add the data for two windows without averaging. It was decided to average even for these methods since the results for 1.0 second and 0.5 second windows are of similar value after averaging and may be numerically compared or plotted together for quick visual comparison.

4.4 Determination of the Set of Ellipses to be Retained and the Percentage of Data Points within an Ellipse

As can be seen from Fig. 4.3, Program AUTOPUFF reads the values of the statistical parameters, defining the set of ellipses under study, from the disk files in which they were stored by STATSMAN. From these values, it determines the enlargement factors (P_{UFF} ; where $0.2 \leq P_{UFF} \leq 3.2$) at which one or more ellipse pairs overlap. After this calculation is complete, each of the unique product terms (Equation 3.4.4) is constructed for the lowest P_{UFF} factor at which the ellipses overlap and the set of minimum elements to be discarded is found. There may be many such sets. The set of minimum elements which is chosen is the first which occurs in the product table. This is a weakness in the analysis procedure since another set may provide larger values of % AVG. The next pair of ellipses to touch, either at the same or next

highest value of P_{UFF} , are then included in the product and a new solution is calculated. For identical products, all but one are discarded and analysis proceeds to the subsequent pair of ellipses. This process continues, considering the ellipses at even higher values of P_{UFF} , until all pairs which overlapped for $P_{UFF} \leq 3.2$ have been included. At this point, for each P_{UFF} factor at which ellipses overlapped, a table has been constructed showing the set of levels to discard in order to retain as many as possible and still have no overlapping.

AUTOPUFF then commences with the lowest value of P_{UFF} and calculates the minimum percentage (% MIN) and average percentage (%AVG) of valid DISTILLED data points which lie within the appropriate ellipses for all non-overlapping ellipses. This process is repeated for successively higher P_{UFF} factors until all have been considered. For higher P_{UFF} factors, the number of discarded levels is greater due to increased overlap and therefore the number of distinct ellipses remaining (#LFT) diminishes. The percentages calculated should gradually, but not necessarily monotonically, increase.

To prevent excessive program execution time and because of computer core limitations, certain restrictions were placed on AUTOPUFF's capabilities. If, at some value of P_{UFF} , the number of discarded ellipses exceeds fifteen, results to that point will be printed out and no higher values of P_{UFF} will be considered. If the number of overlapping pairs of

ellipses exceeds seventy for the range of $0.2 \leq P_{UFF} \leq 3.2$, then analysis will continue with the reduced range of $0.2 \leq P_{UFF} \leq 2.6$. Both of these restrictions will make it difficult to obtain complete results for signal processors for which a large number of overlapping ellipse pairs exist. This is not considered a serious limitation since it is still possible to determine that a particular method is of such low comparative performance as to be of little use.

CHAPTER 5

RESULTS AND DISCUSSIONS

Due to time limitations, the main thrust of this project was to develop a method of analysis and to demonstrate its use, rather than compile extensive data. Only a few experiments, of an exemplary nature, were performed upon one individual. The anatomical data for this person is given in TABLE 5.3.

5.1 The Effect of Electrode Position on the Performance of, and the Relative Performance of, Signal Processors

5.1.1 Results:

A single experiment was performed at each of the four electrode positions P_0 , P_1 , P_2 , and P_3 . Tables 5.1 and 5.2 present the number of force levels which may be defined (with the restrictions that these levels be non-overlapping and that $\%AVG \geq 95\%$) as a function of the electrode position and of the signal processing method chosen. Data windows of 0.5 seconds were used for results presented in TABLE 5.1 while results for 1.0 second data windows are presented in TABLE 5.2.

In certain instances, specifically for the FP and

TABLE 5.1 Number of Levels as a Function of Electrode Position for Various Signal Processors (0.5 second windows)

Electrode Position	SIGNAL PROCESSING METHOD (see TABLE 3.1) and number of levels achieved											AVERAGE NUMBER OF LEVELS*
	SUM	RAVG	FP	SP	HP	QP	\overline{SUM}	\overline{PCC}	\overline{SMSP}	$\overline{SMIP5}$	\overline{SMHP}	
P0	11	11	Poor	10	10	11	11	Less than 8	11	10	10	10.63
P1	14	10	Poor	11	-	10	15	11	12	13	13	12.25
P2	13	13	Poor	11	-	11	13	Less than 9	12	13	13	12.34
P3	14	12	Poor	11	11	12	14	Less than 10	11	13	13	12.50

AVERAGE OVER ALL POSITIONS	13	11.5	-	10.75	10.50	11	13.25	-	11.5	12.25	12.25
RANK OF METHOD	2	4	8	6	7	5	1	8	4	3	3

* Only processing methods for which complete data exists are considered

- Not analyzed

TABLE 5.2 Number of Levels as a Function of Electrode Position for Various Signal Processors (1.0 second windows)

Electrode Position	SIGNAL PROCESSING METHOD (see TABLE 3.1) and number of levels achieved											AVERAGE NUMBER OF LEVELS*
	SUM	RAVG	FP	SP	HP	QP	$\overline{\text{SUM}}$	$\overline{\text{PCC}}$	$\overline{\text{SMSP}}$	$\overline{\text{SMIP5}}$	$\overline{\text{SMHP}}$	
P1	16	14	Poor	13	-	13	16	12	14	15	16	14.3
P2	16	14	Poor	12	-	12	14	11	13	15	16	13.7
P3	16	13	Poor	14	13	14	16	Less than 11	15	15	16	14.88

AVERAGE OVER ALL POSITIONS	16	13.7	Poor	13	13	13	15.3	-	14	15	16	
RANK OF METHOD	1	5	8	6	6	6	2	8	4	3	1	

* Only processing methods for which complete data exists are considered

- Not analyzed

AGE: 25 years
SEX: Male
WEIGHT: 64 Kg.
HEIGHT: 1.68 m.

Girth of upper arm as measured at crest of biceps muscle
(i.e. along the line which connects electrode positions
 P_0 and P_E): 0.30 m

Length of the forearm (measured from tip of elbow to wrist):
0.27 m

Length of upper arm (measured from acromion to tip of elbow):
0.36 m

Distance from tip of elbow to crest of biceps: 0.18 m

TABLE 5.3 Anatomical Data of Subject

\overline{PCC} signal processing methods, results are so inferior that one or more of the analysis limitations (outlined in the latter half of Section 4.4) are exceeded and quantitative results are not obtained. For this reason, some entries are marked "poor". Similarly a full assessment for some other cases is not feasible but it is possible to determine that the number of achievable levels is less than a certain value. For the method HP, assessment was not performed for the P_1 and P_2 electrode positions since these were the first positions studied and, at that time, this method was not yet part of the repertoire of methods.

A further entry in Tables 5.1 and 5.2 is the average of the number of achievable levels over all electrode positions considered. This information is used as a figure of merit to assess or rank the relative performance of each of the signal processing methods.

When determining the number of achievable levels the values of %AVG are rounded to the nearest percent. By considering the average number of force levels it is seen that for the 0.5 second windows, method \overline{SUM} is superior with method SUM a close second. All of the signal processing methods based on P-P amplitude are superior to the power law techniques. Of the power law techniques, RAVG is somewhat superior to QP. For higher powers, the performance deteriorates. \overline{PCC} proves to be a poor method of analysis.

Method \overline{SUM} is considered as the superior method for another reason. It provides the largest number of

distinct levels with a total of 15 levels at P_1 . P_1 was chosen as the superior electrode site since it provided absolutely the largest number of levels.

5.1.2 Discussion:

As noted, there is no marked difference in the performances of SUM and $\overline{\text{SUM}}$. The fact that signal inversion causes no appreciable change is of particular interest in regard to those methods measuring P-P amplitude. If an AP is detected at the surface having the waveform as shown in Fig. 2.1(a) (where the initial peak is positive), the peak detector used in this analysis (Section 3.4) will measure the P-P amplitude of the action potential correctly. If the wave form is inverted, the peak detector will measure not the AP's P-P amplitude but the P-P amplitude between two successive AP's. Thus, if all AP's are not inverted it is to be expected that SUM should be superior to $\overline{\text{SUM}}$. However, since both methods produce equivalent results, it is possible that the number of action potentials detected with a measured initial positive peak is equal to the number detected with a measured initial negative peak. More complex variations in the wave form could also occur. The use of a more sophisticated peak detector, which measures both positive and negative going peaks which are distinct, may improve results. Such a peak detector would reliably measure P-P amplitudes for inverted and non-inverted AP's.

The observation, that electrode position P_0 is

inferior, is of interest, since it is located at the crest of the biceps muscle and it is the position most commonly used by researchers. This point merits further investigation with a more complete set of experiments.

Comparison of Tables 5.1 and 5.2 indicates that more force levels are definable using 1.0 second windows than with 0.5 second windows. The higher SNR's of the processed EMG attained by using increased smoothing windows are responsible for this increase in the number of force levels. Results for the 1.0 second windows also show that the methods based on P-P amplitude are still superior to the power law methods although ranking is somewhat changed.

Of all the P-P methods, $\overline{\text{SUM}}$ or SUM provide not only the best results but are easiest to implement in software since it is not necessary to calculate a power of the P-P amplitude. Likewise, RAVG gives the best performance of all the power law processors and is easily implemented.

5.1.3 Qualitative Observations on the Variation of the EMG with Wrist Pronation and Electrode Position:

A qualitative, preliminary investigation of the effect of wrist pronation or supination on the EMG showed it to be a strong function of electrode position. Utilizing a storage oscilloscope, visual estimates of the EMG were made while the subject supported a 2.4 Kg., hand-held weight by isometric contraction of the upper arm muscles. Position P_0 showed the greatest variation between signals taken with the

wrist pronate or supine. At electrode position P_2 , a signal was obtained which appeared to be relatively invariant with wrist pronation. As the electrode position advanced from P_0 to P_3 , an increase in the EMG was observed when the extensors were active. This could be due to increased cross-talk as the flexor electrode moves ever more proximal to the extensors. This hypothesis was supported by the observation of an increased antagonist activity for a given force level as the flexor electrode advanced from P_0 to P_3 in the experiments described in Section 5.1.1.

The smaller variation observed in EMG at position P_2 is not so surprising when the physiology and anatomy of the musculature is examined. Basmajian [13] found that during flexion the BR was primarily active with the wrist pronate while both BB and BR were active with the wrist supine. The degree of activity of each muscle showed variation among individuals. Fig. 2.2 illustrates that the BR is located beneath the BB and on the lateral aspect of the upper arm. Electrode position P_0 should permit monitoring of the EMG mainly due to the BB but some feed through from the BR is expected. This feed through should be increased at position P_1 . At position P_2 where the electrodes are proximal to both muscles, the observed EMG is expected to consist of a more evenly weighted summation of the BB and BR EMG's.

This preliminary study suggests that one of the electrode positions (P_2) provides more information concerning the net activity of the two flexors than any of the others.

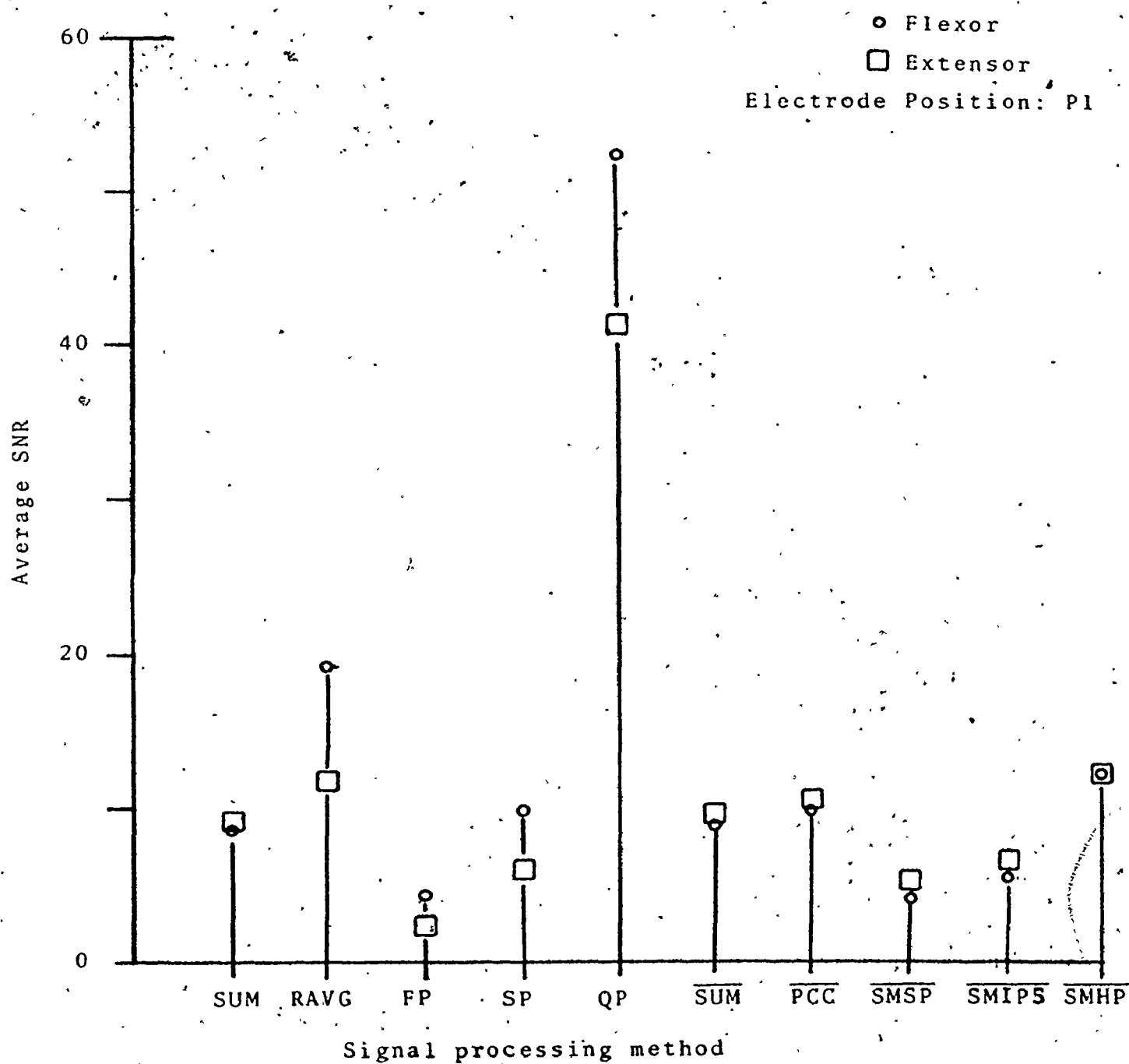
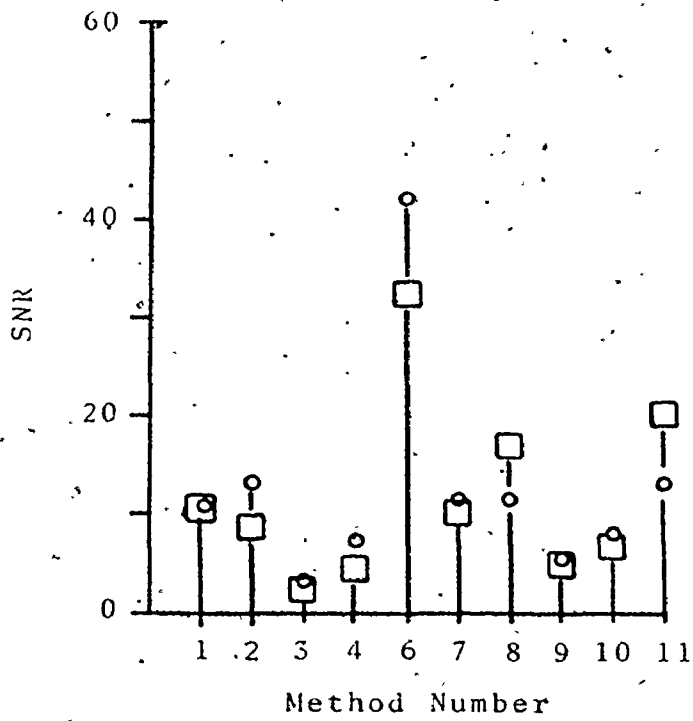


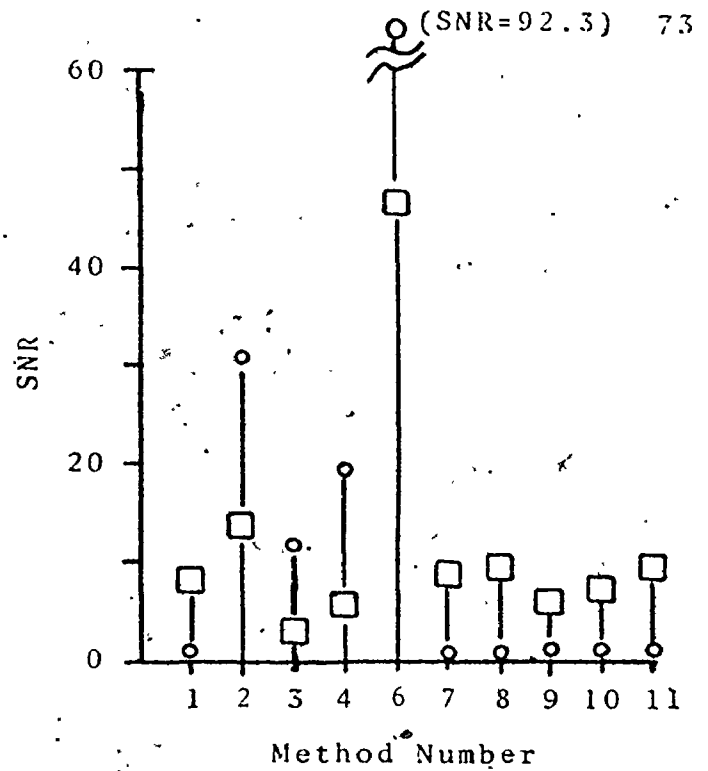
Fig. 5.1 Signal to noise ratios

		Signal Processing Method									
		SUM	RAVG	FP	SP	QP	$\overline{\text{SUM}}$	$\overline{\text{PCC}}$	$\overline{\text{SMSP}}$	$\overline{\text{SMIP5}}$	$\overline{\text{SMHP}}$
RANK		6	2	10	7	1	5	4	9	8	3

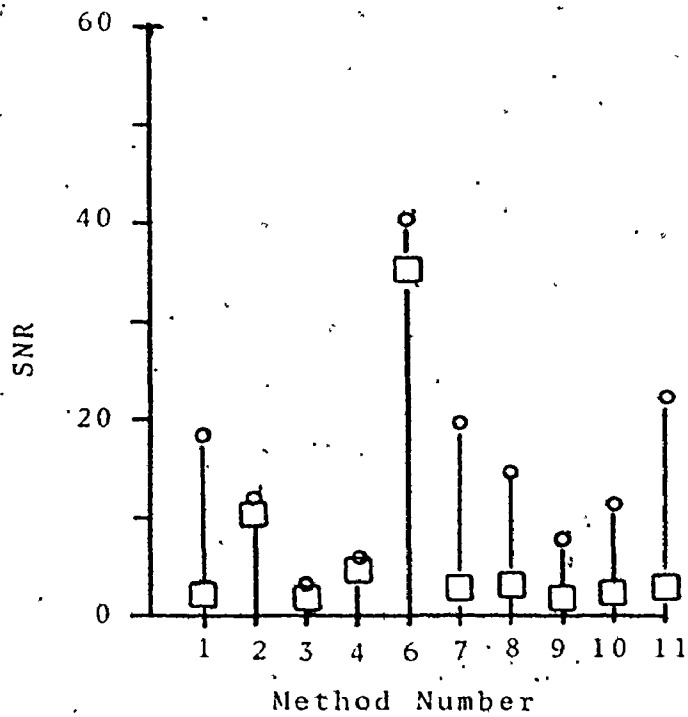
TABLE 5.4 Ranking of processors using SNR's



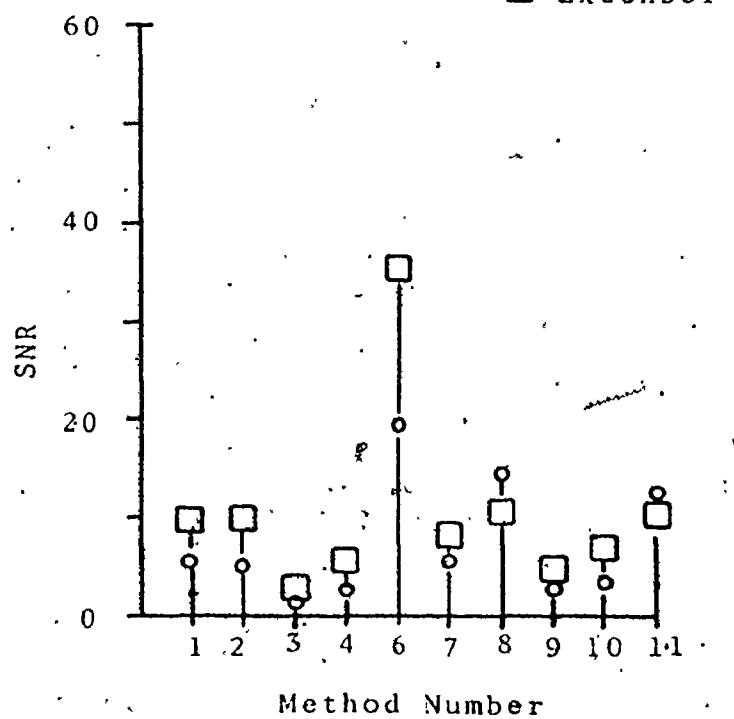
(a) Net force: -7.6 Kg.



(b) Net force: -1.6 Kg.



(c) Net force: +1.0 Kg.



(d) Net force: +6.0 Kg.

Fig. 5.2 SNRs at Various Force Levels (electrode position P1)

○ Flexor
□ Extensor

This explains why a variation in the quality of the results as a function of electrode position can be expected even when the wrist is maintained supine at all times.

5.2. The Use of SNR's to Rank the Performance of Signal Processing Methods

The SNR's, for both the flexor and extensor EMG's, of each of ten signal processors was evaluated for nine different force levels. The force level numbers of those force levels considered are 1, 4, 7, 9, 11, 14, 18, 21, and 23. (TABLE 4.3). The average SNR over all nine force levels was calculated for each agonist for each of the processors (Fig. 5.1). The SNR's of each of the processors for four different force levels is presented in Fig. 5.2. To rank the relative performance of the signal processors, the mean, of the average ~~SNR's~~ for each agonist, was used (TABLE 5.4).

Considerable disagreement is discovered between the ranking of processors on the basis of SNR's as compared to the ranking on the basis of definable force levels (TABLE 5.1). The SNR method is poor since the sensitivity of the processed signals to changes in the EMG is not considered. The number of definable force levels is a more useful parameter since it is inherently dependent on both SNR's and on the sensitivity. deBruin ([4] private communication) has suggested a promising technique for ranking of processors. He defines a "Figure of Merit" which is dependent upon both the SNR and the slope of the processed output versus the net

force exerted.

5.3 Sensitivity of Parameters to Electrode Placement

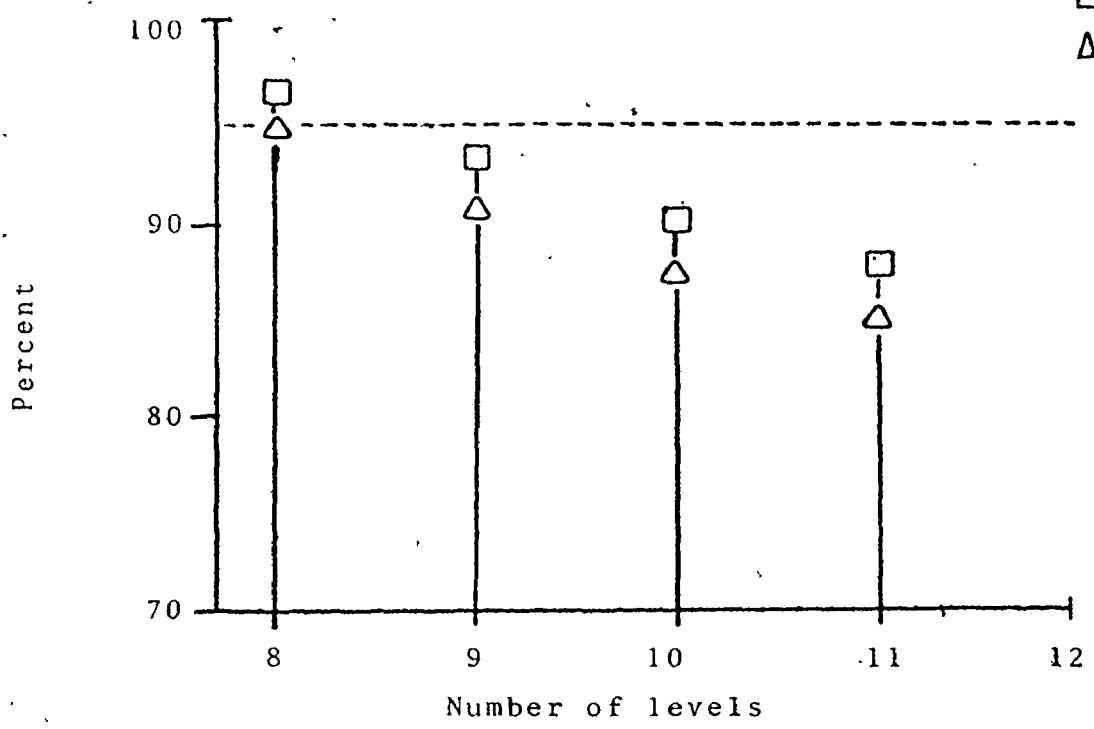
Although it may be possible to define roughly the same number of levels at various electrode positions, these levels may be entirely different. To determine how accurately electrodes must be positioned in order to achieve reproducible results, the sensitivity of the processed EMG to electrode position must be determined.

To investigate this, the processed data for electrode positions P_0 , P_1 and P_2 were considered together. The statistical parameters representing this aggregate were calculated and the number of levels was evaluated using 0.5 second windows. Only method $\overline{\text{SUM}}$ and RAVG were considered since they are of special interest as previously discussed.

It was found that a total of ten levels were definable for method $\overline{\text{SUM}}$ while RAVG permitted the definition of eight levels. (Fig. 5.3). The number of levels definable with the restriction that $\%AVG \geq 90\%$, was 11 levels for $\overline{\text{SUM}}$ and 10 levels for RAVG.

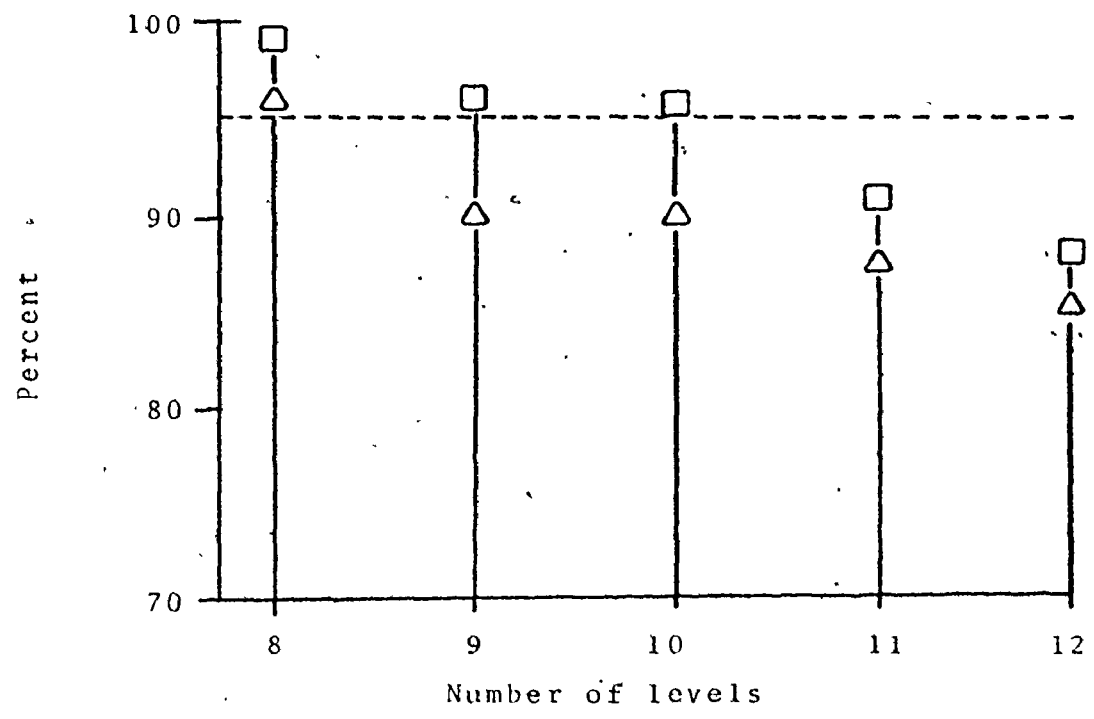
These results are compared with those obtained when the data for many experiments performed at one location are combined. (Section 5.4, TABLE 5.7). It is seen that the decrease in the number of definable levels is similar in both cases. As data from only one experiment per electrode site is combined the results can only be considered preliminary, but it is indicated that these signal processing methods are

□ - %AVG
△ - %MIN



(a)

□ - %AVG
△ - %MIN



(b)

Method: \overline{SUM}
Window: 0.5 sec.
Positions: $P_0, P_I,$ and P_2

Fig. 5.3 Combined data for several electrode positions

relatively insensitive to electrode placement.

The observations that electrode position P_0 is inferior and that the results are not highly sensitive to electrode position imply that although the SNR's for various force levels may vary with electrode placement, the means do not.

5.4 Combined Data of Several Experiments

5.4.1 Results:

A total of six similar experiments were performed. These were conducted at the best electrode position (P_1) using methods $\overline{\text{SUM}}$ and RAVG with both 0.5 and 1.0 second windows. The DISTILLED data for all experiments was combined in one overall analysis.

A full computer printout of the statistical parameters for this analysis is presented in TABLE 5.5 using method $\overline{\text{SUM}}$ with a 0.5 second window. The values associated with each of the 23 force levels of level number 1 are also indicated. Most of the FORTRAN symbols used in the headings are similar to the mathematical symbols used in this thesis with the constraint that no subscripts and only capital letters are allowed. Thus the FORTRAN symbol for A_{LPH3TN} is ALPH3TN, S_{LOP} is represented by SLOPE, N_{TCPT} by INTERCEPT, r by R and so forth. AMNAFF is the mean measured force in kilograms for the force level over all experiments. ILCNT is used merely for bookkeeping. The number of data windows analyzed per force level is N. In some cases, the data for a force

ILCNT N	I	R	ANGL 1	SLOPE	INTERCEPT
MEANB		SDVB	SDVEN	ALPH3B	ALPH4B
MEANT		SDVT	SDVTN	ALPH3T	ALPH4T
ALPH3BN		ALPH4BN	AMNAFF	ALPH3TN	ALPH4TN
1 240	1	0.2082E -1	-0.7069E -2	0.7720E -1	0.1057E 2
0.2149E	1	0.4469E 0	0.4468E 0	0.8605E 0	0.2860E 1
0.1073E	2	0.1657E 1	0.1657E 1	0.4590E 0	0.2838E 1
0.8916E	0	0.2908E 1	-0.7559E 1	0.4590E 0	0.2839E 1
3 240	2	-0.1965E 0	0.7854E -1	-0.4791E 0	0.9105E 1
0.1758E	1	0.3594E 0	0.3513E 0	0.8907E 0	0.3350E 1
0.8263E	1	0.8764E 0	0.8796E 0	0.2961E -1	0.3164E 1
0.9996E	0	0.3556E 1	-0.6585E 1	0.3090E -1	0.3129E 1
5 240	3	-0.3756E 0	0.1186E 0	-0.1267E 1	0.8485E 1
0.1426E	1	0.2226E 0	0.2049E 0	0.5914E 0	0.3099E 1
0.6678E	1	0.7510E 0	0.7560E 0	0.3046E 0	0.2833E 1
0.3414E	0	0.3159E 1	-0.5591E 1	0.2899E 0	0.2801E 1
7 240	4	0.8427E -1	-0.6283E -1	0.2526E 0	0.5248E 1
0.1046E	1	0.1705E 0	0.1705E 0	0.7116E 0	0.2879E 1
0.5513E	1	0.5112E 0	0.5112E 0	-0.7102E -1	0.2654E 1
0.7707E	0	0.3055E 1	-0.4593E 1	-0.7213E -1	0.2680E 1
9 240	5	0.2335E -1	-0.7069E -2	0.9995E -1	0.3628E 1
0.6565E	0	0.1143E 0	0.1143E 0	0.1552E 1	0.6379E 1
0.3694E	1	0.4892E 0	0.4892E 0	0.1337E 0	0.2573E 1
0.1585E	1	0.6507E 1	-0.3602E 1	0.1331E 0	0.2576E 1
11 240	6	0.1726E 0	-0.3063E -1	0.1026E 1	0.2270E 1
0.4876E	0	0.7082E -1	0.6973E -1	0.8073E 0	0.5447E 1
0.2770E	1	0.4208E 0	0.4209E 0	0.7312E 0	0.3608E 1
0.8538E	0	0.5466E 1	-0.3102E 1	0.7264E 0	0.3605E 1
13 240	7	0.5652E -1	-0.1335E -1	0.3084E 0	0.2041E 1
0.3509E	0	0.5526E -1	0.5517E -1	0.6098E 0	0.3776E 1
0.2150E	1	0.3015E 0	0.3015E 0	-0.1333E 0	0.2744E 1
0.7069E	0	0.4116E 1	-0.2601E 1	-0.1310E 0	0.2742E 1
15 240	8	0.1779E 0	-0.1257E -1	0.2520E 1	0.7466E 0
0.1845E	0	0.3044E -1	0.2995E -1	-0.9562E -1	0.2645E 1
0.1212E	1	0.4311E 0	0.4311E 0	0.3902E 0	0.2310E 1
-0.1248E	0	0.2695E 1	-0.2103E 1	0.3900E 0	0.2310E 1

TABLE 5.5 Statistical values for combined data for six experiments (computer print-out)

ILCNT N	I	R	ANGL I	SLOPE	INTERCEPT
MEANB		SDVB	SDVEN	ALPH3B	ALPH4B
MEANT		SDVT	SDVTN	ALPH3T	ALPH4T
ALPH3EN		ALPH4EN	AMNAFF	ALPH3TN	ALPH4TN
17 240	9	-0.5798E -1	-0.3725E -7	-0.3059E 0	0.3842E 0
0.5730E -1		0.2800E -1	0.2800E -1	0.4822E 0	0.2889E 1
0.3667E 0		0.1477E 0	0.1477E 0	0.1001E 1	0.3917E 1
0.4822E 0		0.2889E 1	-0.1601E 1	0.1001E 1	0.3917E 1
19 240	10	-0.6942E -1	0.5498E -2	-0.8194E 0	0.3802E -1
0.2709E -2		0.5488E -2	0.5475E -2	0.2170E 1	0.8209E 1
0.3580E -1		0.6477E -1	0.6478E -1	0.2323E 1	0.7887E 1
0.2163E 1		0.8235E 1	-0.1106E 1	0.2323E 1	0.7888E 1
21 240	11	-0.1728E 0	-0.3691E -1	-0.3313E -1	0.4805E -1
0.4315E 0		0.3170E 0	0.3172E 0	0.4824E 0	0.1853E 1
0.3376E -1		0.6080E -1	0.5985E -1	0.2128E 1	0.6903E 1
0.4839E 0		0.1853E 1	-0.7888E 0	0.1957E 1	0.6470E 1
23 240	12	-0.3610E -1	-0.2278E -1	-0.1713E -1	0.6327E -1
0.1118E 1		0.1574E 0	0.1575E 0	0.2327E 0	0.2383E 1
0.4411E -1		0.7470E -1	0.7464E -1	0.2051E 1	0.6553E 1
0.2349E 0		0.2396E 1	0.9846E -2	0.2042E 1	0.6572E 1
LN B(1,	13)=	25	IRJECT=	15	
25 225	13	-0.2703E -1	-0.2356E -1	-0.1053E -1	0.9109E -1
0.1933E 1		0.2030E 0	0.2030E 0	0.9514E 0	0.4835E 1
0.7074E -1		0.7905E -1	0.7904E -1	0.1519E 1	0.4348E 1
0.9544E 0		0.4847E 1	0.4840E 0	0.1481E 1	0.4249E 1
27 240	14	0.1735E 0	0.4712E -1	0.4123E -1	0.3144E -2
0.2593E 1		0.3266E 0	0.3269E 0	0.8139E 0	0.3498E 1
0.1101E 0		0.7764E -1	0.7640E -1	0.1527E 1	0.4773E 1
0.8082E 0		0.3495E 1	0.9881E 0	0.1559E 1	0.4991E 1
ILN B(1,	15)=	29	IRJECT=	1	
29 239	15	0.4409E 0	0.7854E -1	0.8133E -1	-0.8994E -1
0.3260E 1		0.4218E 0	0.4233E 0	0.1073E -1	0.2773E 1
0.1752E 0		0.7781E -1	0.6964E -1	0.1278E 1	0.5117E 1
0.2707E -1		0.2774E 1	0.1484E 1	0.1207E 1	0.4896E 1
31 240	16	0.1939E 0	0.4791E -1	0.4688E -1	0.8755E -1
0.3751E 1		0.3840E 0	0.3844E 0	-0.1202E -1	0.2367E 1
0.2634E 0		0.9286E -1	0.9099E -1	0.9541E 0	0.3516E 1
-0.7122E -2		0.2371E 1	0.1985E 1	0.1016E 1	0.3713E 1

TABLE 5.5 Cont'd

ILCNT N	I	R	ANGL I	SLOPE	INTERCEPT
MEANB.		SDVB	SDVEN	ALPH3B	ALPH4B
MEANT		SDVT	SDVTN	ALPH3T	ALPH4T
ALPH3BN		ALPH4BN	AMNAFF	ALPH3TN	ALPH4TN
33 240	17	0.2733E -1	0.1863E -8	0.3249E -2	0.3222E 0
0.4435E	1	0.6698E 0	0.6698E 0	0.3373E 0	0.2971E 1
0.3366E	0	0.7965E -1	0.7965E -1	0.1192E 0	0.2577E 1
0.3372E	0	0.2972E 1	0.2484E 1	0.1194E 0	0.2577E 1
35 240	18	-0.1750E 0	-0.2325E -1	-0.2291E -1	0.5228E 0
0.4941E	1	0.7241E 0	0.7243E 0	0.7522E 0	0.3266E 1
0.4096E	0	0.9477E -1	0.9328E -1	0.8193E 0	0.3682E 1
0.7515E	0	0.3266E 1	0.2985E 1	0.8042E 0	0.3767E 1
37 240	19	-0.1033E 0	-0.1178E -1	-0.1074E -1	0.6609E 0
0.6282E	1	0.9665E 0	0.9665E 0	0.1042E 1	0.3892E 1
0.5935E	0	0.1004E 0	0.9987E -1	0.3791E 0	0.2907E 1
0.1042E	1	0.3892E 1	0.3982E 1	0.3130E 0	0.2904E 1
39 240	20	-0.1735E 0	-0.1257E -1	-0.1236E -1	0.8744E 0
0.7853E	1	0.1588E 1	0.1588E 1	0.6910E 0	0.2687E 1
0.7773E	0	0.1132E 0	0.1115E 0	-0.1393E 0	0.2665E 1
0.6905E	0	0.2685E 1	0.4974E 1	-0.1976E 0	0.2796E 1
41 240	21	0.2249E -1	0.1863E -8	0.1274E -2	0.9629E 0
0.1018E	2	0.2513E 1	0.2513E 1	0.5761E 0	0.2047E 1
0.9759E	0	0.1423E 0	0.1423E 0	-0.5926E -1	0.2733E 1
0.5761E	0	0.2047E 1	0.5972E 1	-0.5920E -1	0.2731E 1
43 240	22	0.1755E 0	0.7854E -2	0.7966E -2	0.1210E 1
0.1331E	2	0.3869E 1	0.3869E 1	0.1205E 1	0.3906E 1
0.1316E	1	0.1757E 0	0.1729E 0	-0.3277E 0	0.3209E 1
0.1206E	1	0.3907E 1	0.7970E 1	-0.3290E 0	0.3063E 1
45 240	23	0.6767E -1	-0.3725E -7	0.3564E -2	0.1812E 1
0.1906E	2	0.5749E 1	0.5749E 1	0.1514E 1	0.6878E 1
0.1880E	1	0.3028E 0	0.3028E 0	0.3322E 0	0.2928E 1
0.1514E	1	0.6879E 1	0.9951E 1	0.3324E 0	0.2926E 1

TABLE 5.5 Cont'd

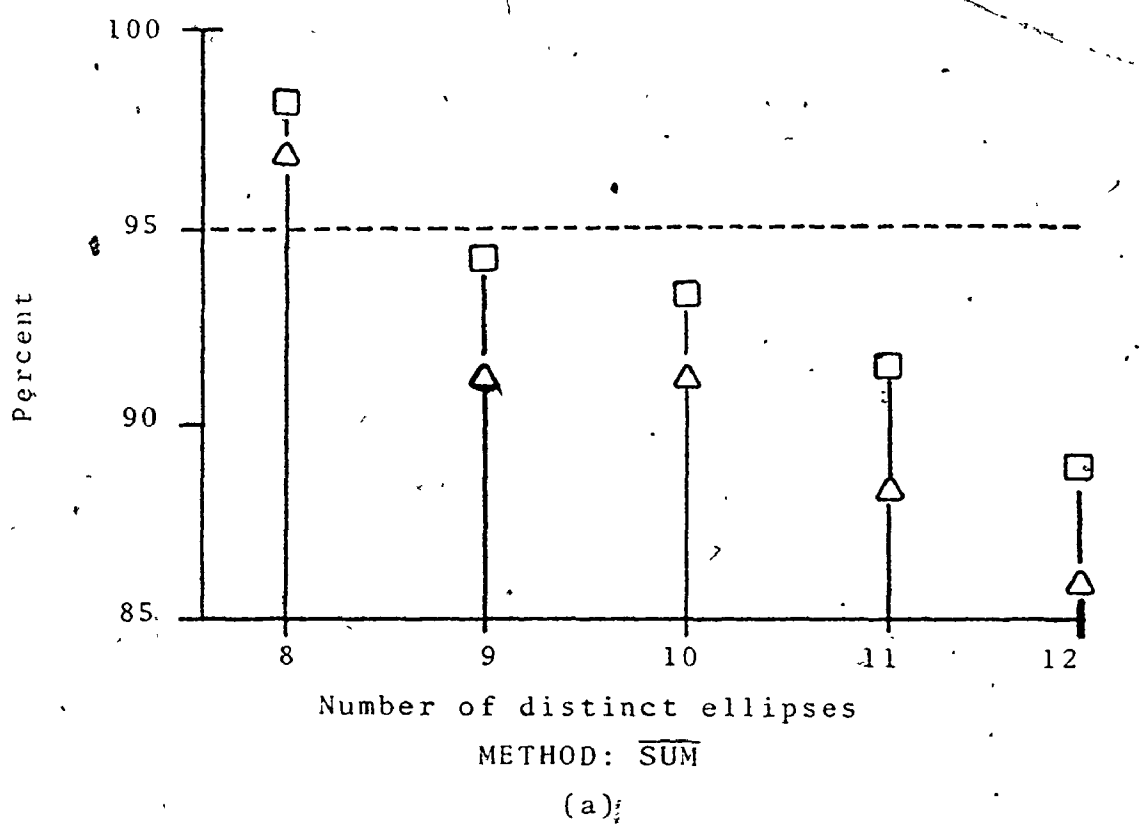
level was rejected for reasons presented in Section 4.3. The number of rejected windows (IRJECT) is indicated as well.

Program AUTOPUFF was used to determine the number of definable levels. A computer printout of the results is presented in TABLE 5.6 using method $\overline{\text{SUM}}$ with 0.5 second windows. %AVG and %MIN as a function of the number of definable levels are to be found in Fig. 5.4 and 5.5 using methods RAYG and $\overline{\text{SUM}}$ for both 0.5 and 1.0 second windows. A plot of the solution set of ellipses for $\overline{\text{SUM}}$ (0.5 second window) is given in Fig. 5.6.

A normalization technique was also considered. M_{EANT} for level #5 (-3.6 Kg.) and M_{EANB} for level #18 (+3.0 Kg.) for each experiment were used to normalize the TRICEPS and BICEPS data respectively. The normalized data for each of the six experiments was then combined and %AVG and %MIN, as a function of level number, were determined, using method $\overline{\text{SUM}}$ with 0.5 second windows (Fig. 5.7).

5.4.2 Discussion:

The values of A_{LPH3BN} and A_{LPH3TN} indicate a marked skewedness in the distributions. Since A_{LPH4TN} and A_{LPH4BN} often differ appreciably from 3.0, some distributions must be significantly more or less peaked than a normal distribution. Thus these distributions can not be described as normal. This could indicate that insufficient data to approach limiting values has been acquired. For this reason,



□ - %AVG
△ - %MIN

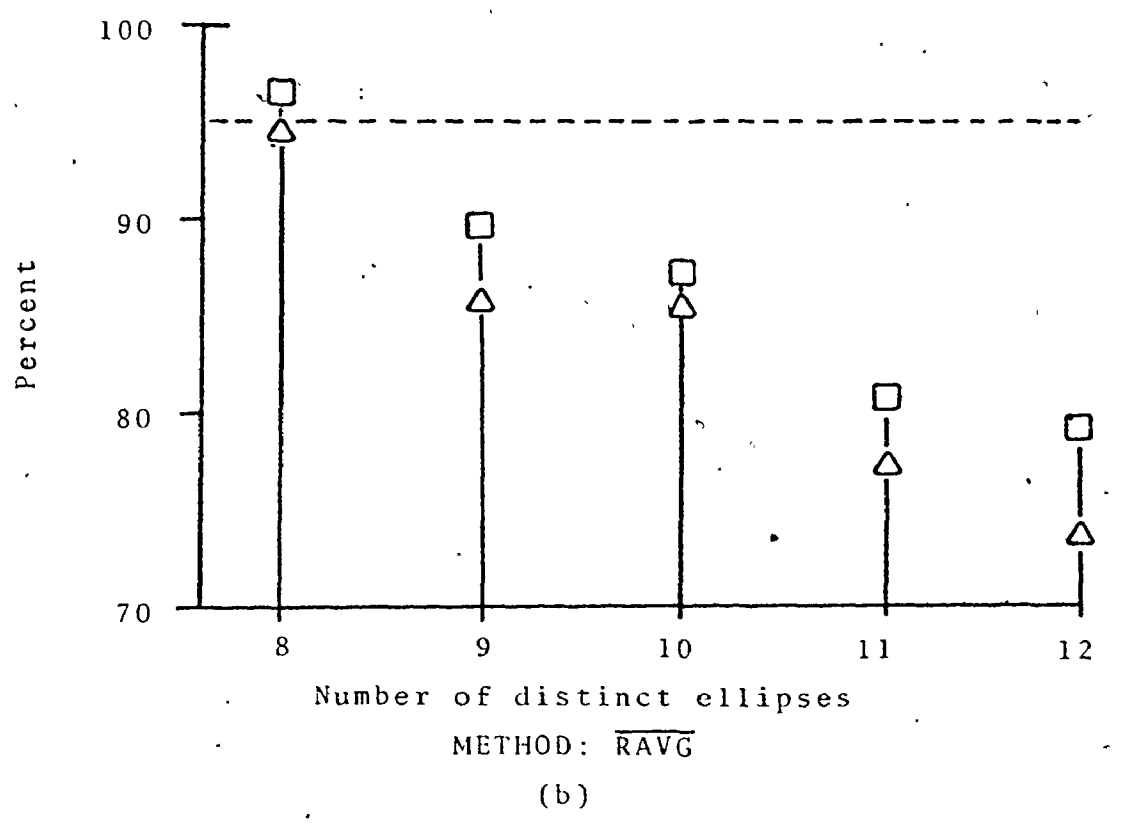


Fig. 5.4 Combined data for several experiments (0.5 second windows)

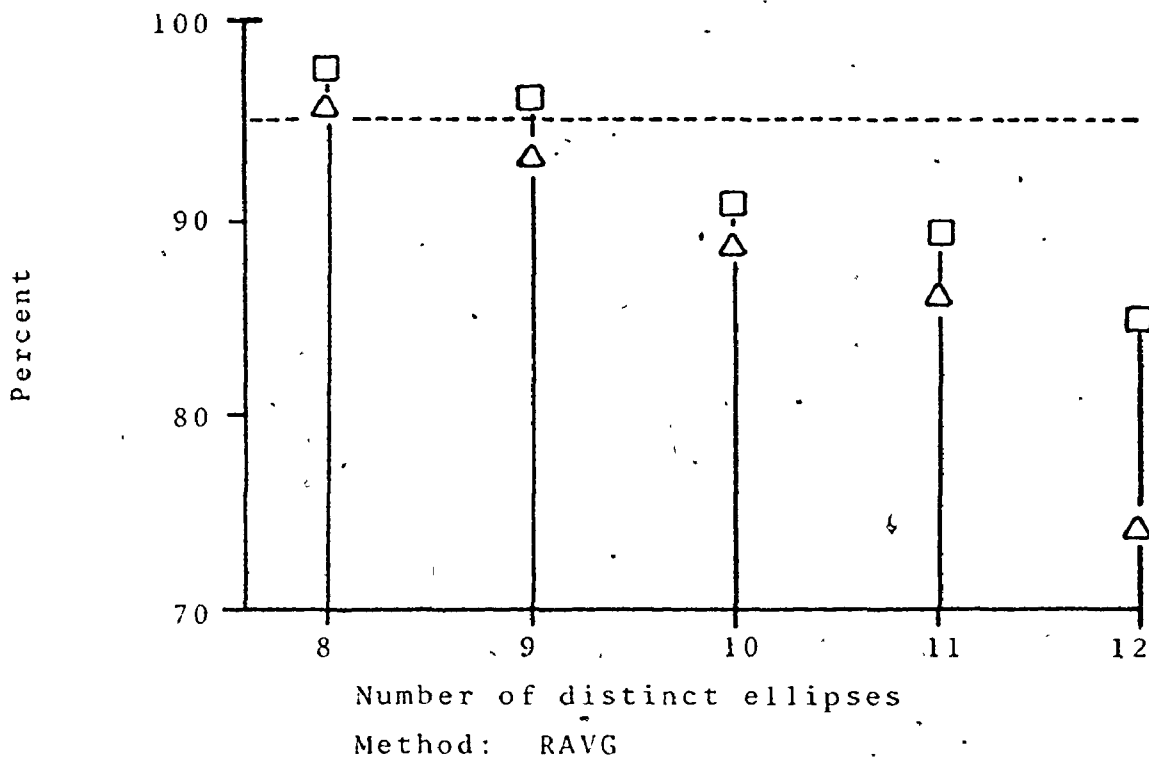
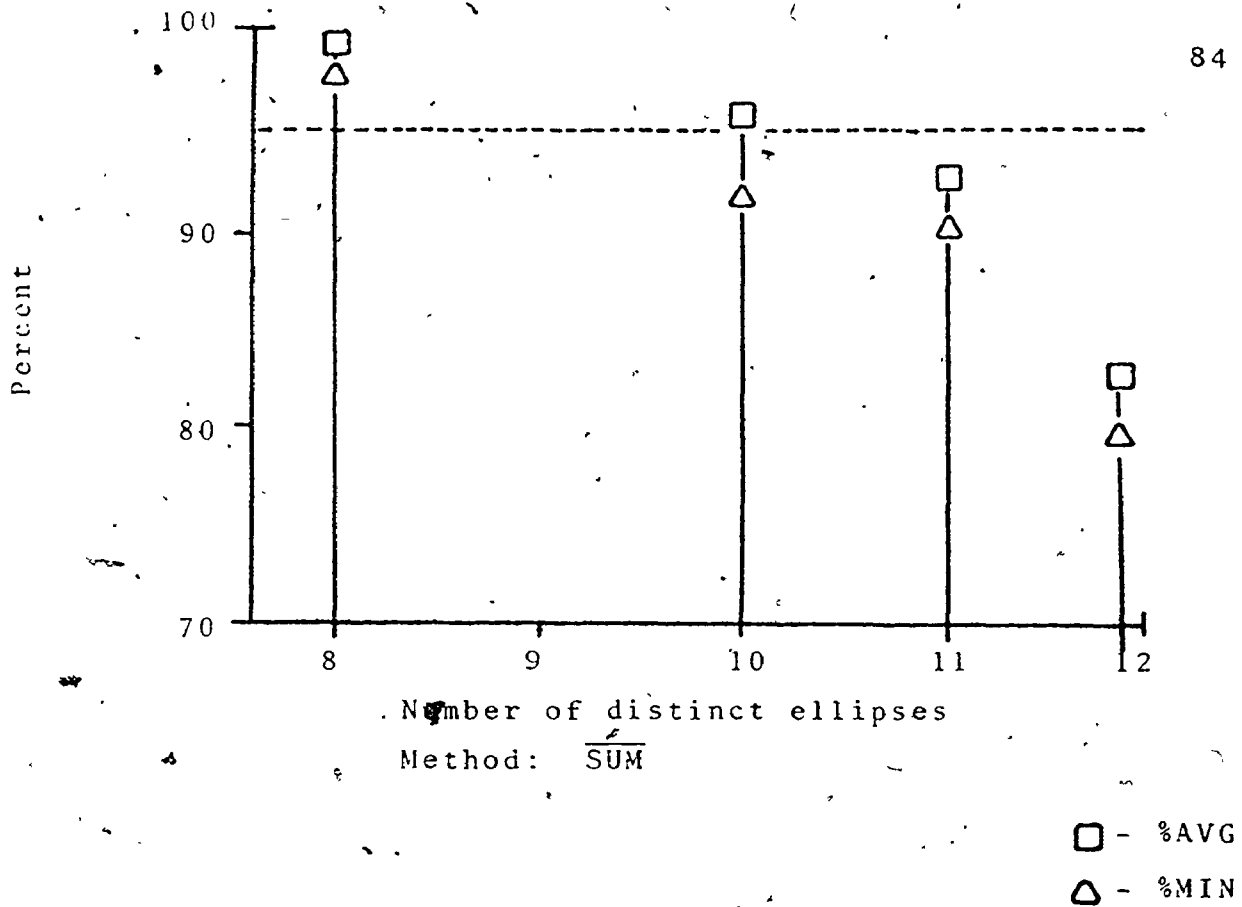


Fig. 5.5 Combined data for several experiments (1.0 second windows)

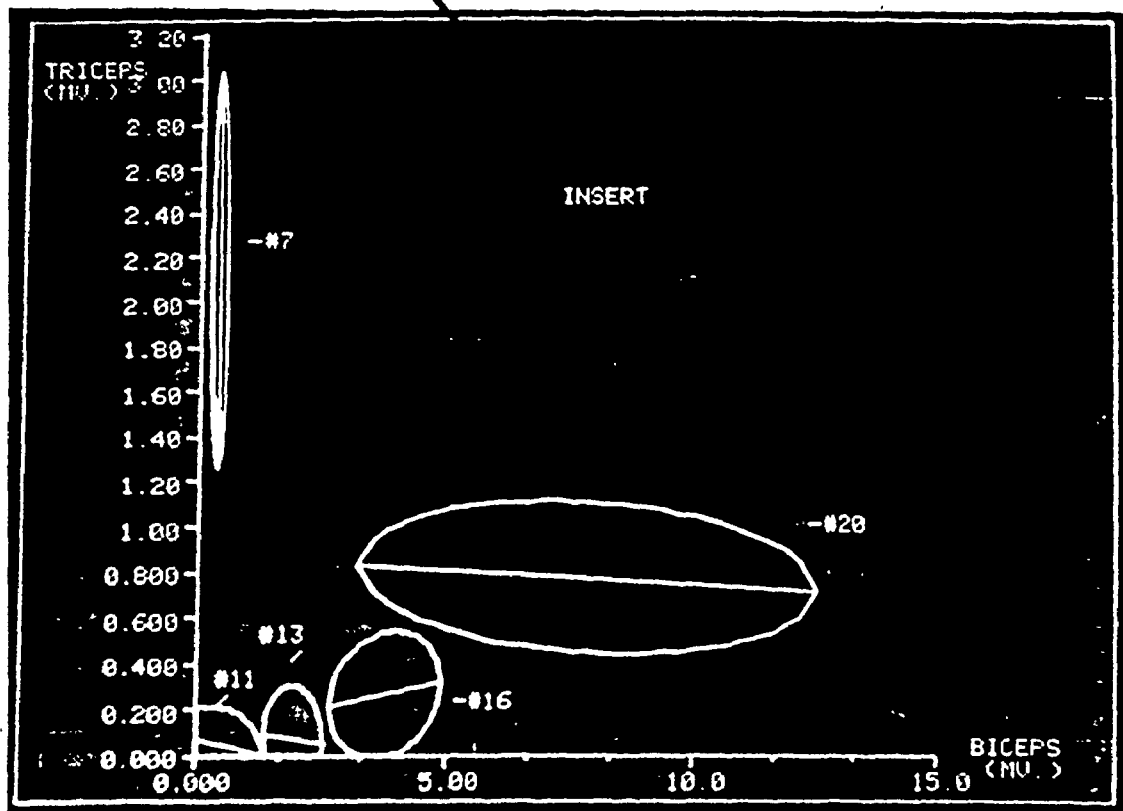
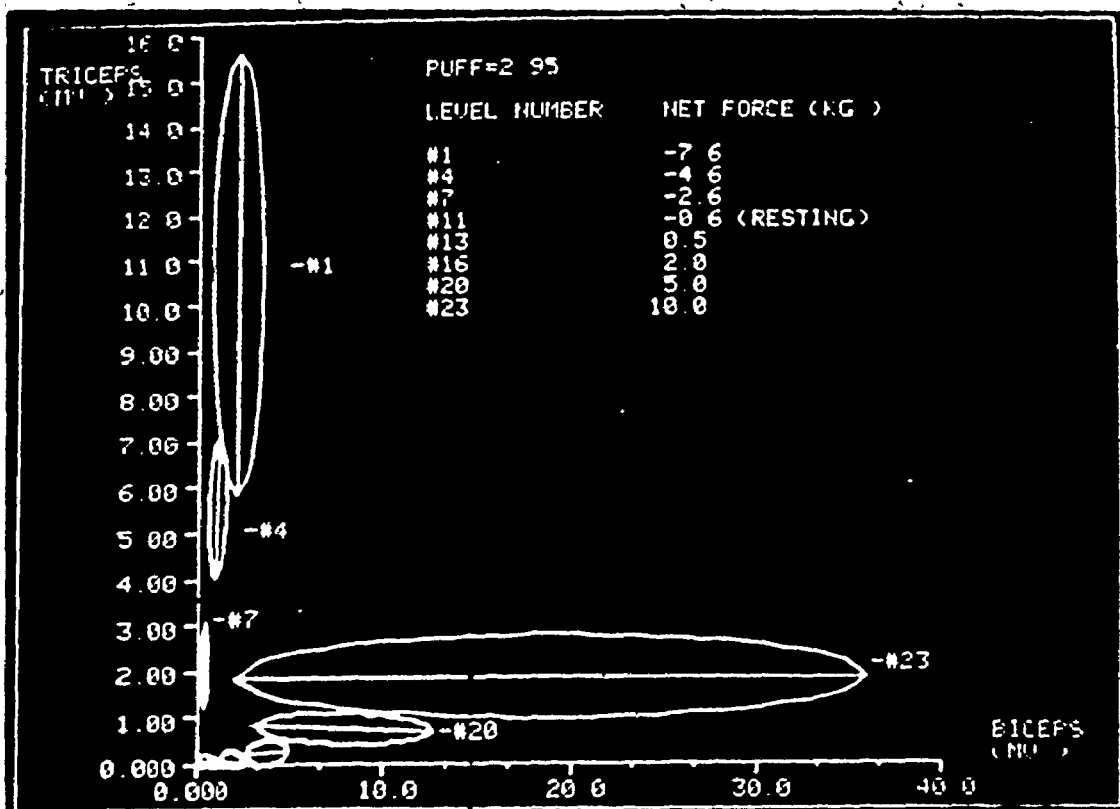


Fig. 5.6 Plot of Solution Set of Ellipses

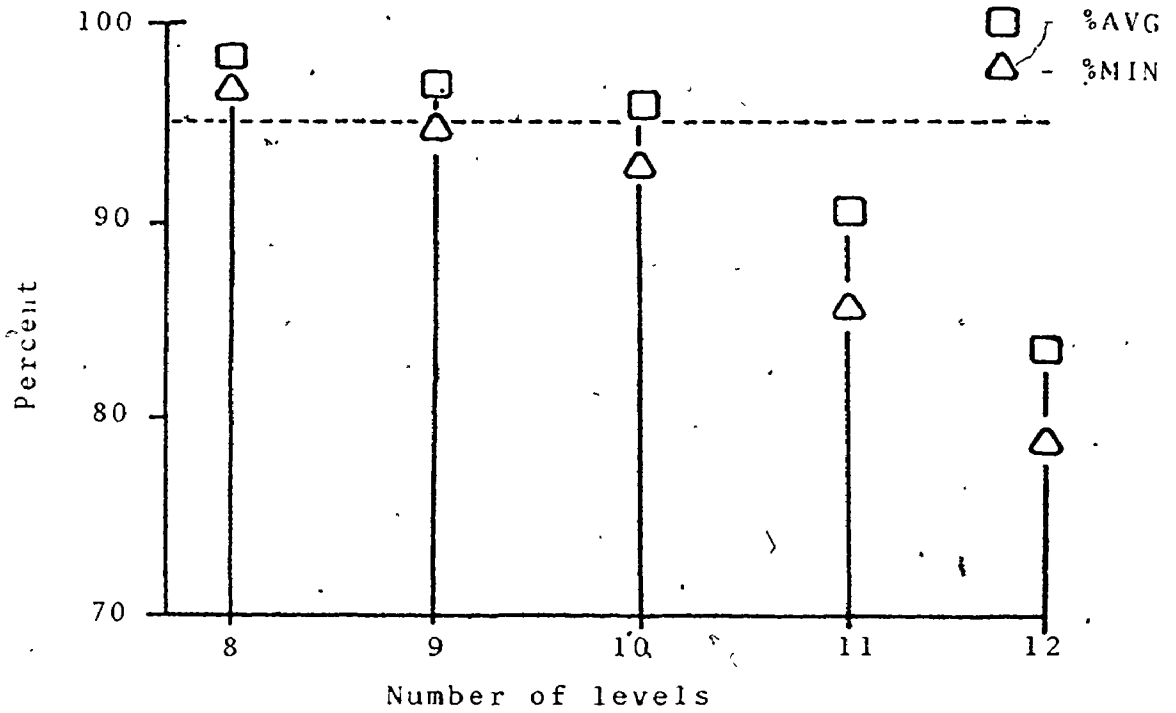


Fig. 5.7 Results for normalized $\overline{\text{SUM}}$ (0.5 second windows)

Window Duration (SECONDS)	%AVG	SIGNAL PROCESSING METHOD		
		$\overline{\text{SUM}}$	Normalized $\overline{\text{SUM}}$	RAVG.
0.5	90	11	11	9
	95	8	10	8
1.0	90	11	---	10
	95	10	---	9

TABLE 5.7 Number of levels for combined data of six experiments

the aggregate data for six experiments can not be considered final.

When the data of a single experiment is examined, fifteen levels can be defined whereas for six combined experiments, only eight levels are found. This large deterioration indicates that the samples for one experiment are not, in general, representative of the overall population. Furthermore, it was observed that within one experiment, appreciable differences can exist between results for two ten second sampling sequences. This variation indicates that some other variable(s) exist which is not well controlled. As can be seen in Fig. 5.8, two ten second sequences in one experiment at a single force level can produce different and distinct data clusters. Fig. 5.9 presents two ellipses denoting the data for two of the six experiments considered. A marked difference between the ellipses is seen.

We hypothesize that the uncontrolled variable is the level of activity of the antagonist. Since each ten second interval usually shows a clear data cluster with no marked linear trait, as indicated by regression coefficient, it seems plausible that the agonist pair establishes and maintains a certain balance of muscle activity over each sampling sequence. The fluctuations in values over one ten second interval would then largely be due to random fluctuations in the processor outputs caused by the short filter time constant. Different data clusters would be observed for sampling sequences if a slightly different agonist

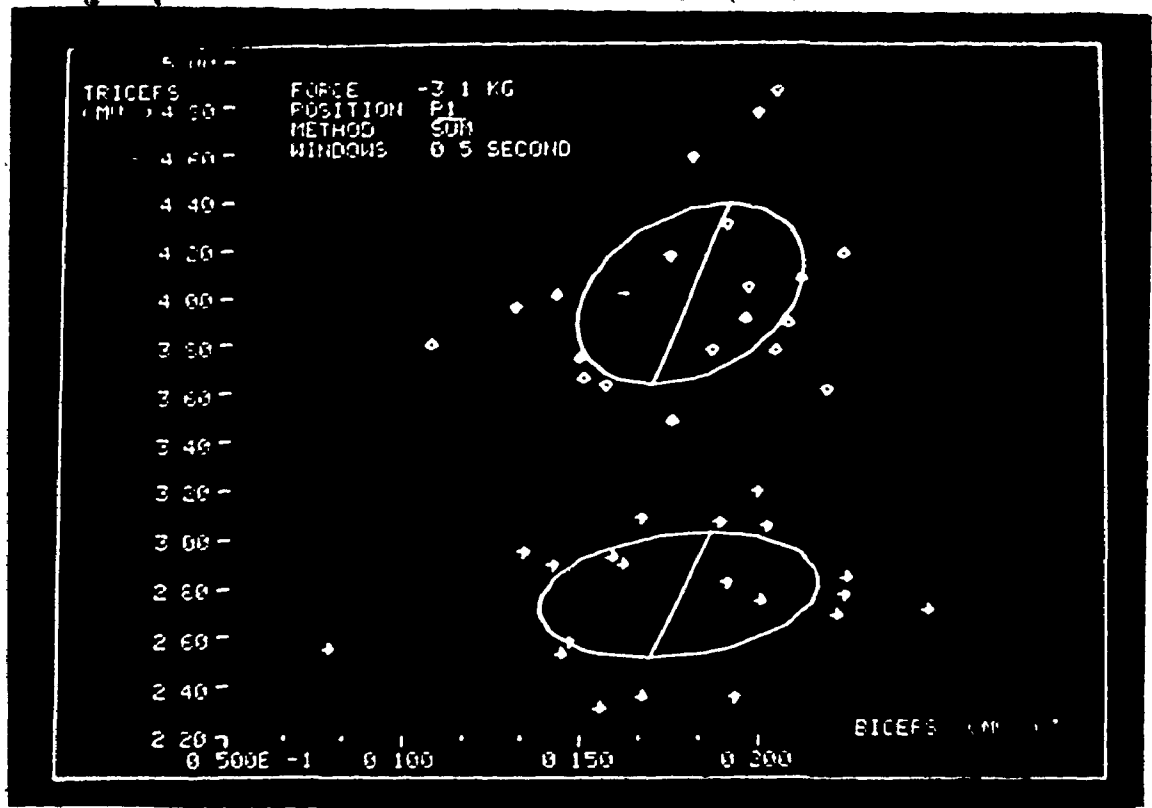


Fig. 5.8 Ellipses for Two Sampling Sequences (method \overline{SUM})

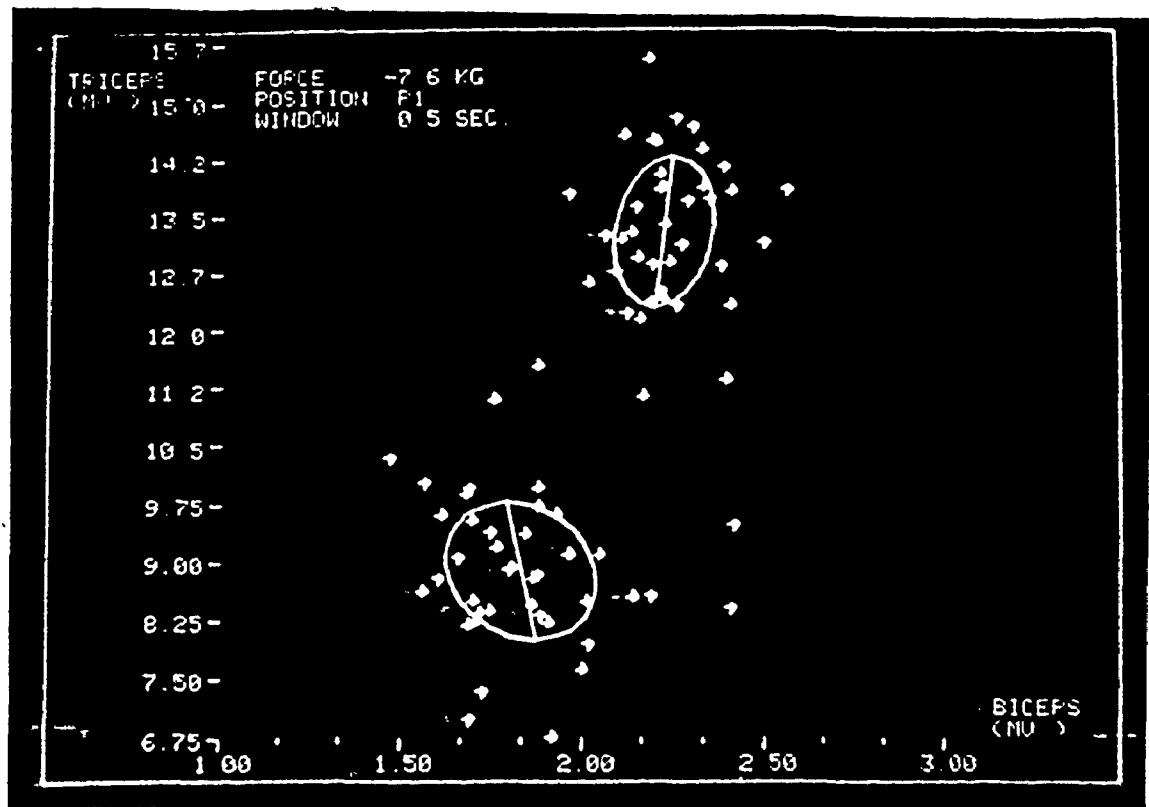


Fig. 5.9 Ellipses for Two Experiments (method \overline{SUM})

equilibrium is established. In a few instances, two clusters of data were recognizable for one sampling sequence, with a small portion of the data scattered in the transition region between the two clusters.

The severe deterioration of results when several experiments are combined could be due to physiological or emotional changes in the subject on a day to day basis. Our subject complained of tension during the period when the six experiments were performed. Although he complained of no muscular fatigue, he found a greater difficulty than usual in maintaining a constant force. Periodically, he had some slight muscle twitching.

These problems did not exist during an earlier set of experiments with the same subject. In these early experiments, analysis did not involve the use of the ellipse of minimum area. Rather, the ellipse chosen had its major axis along the line of linear regression to the data. This ellipse is often significantly larger than the ellipse of minimum area. Surprisingly despite the use of larger ellipses, it was found that twelve levels with $\%AVG = 96.25\%$ and $\%MIN = 92.1\%$ could be defined. This is a considerable improvement when compared to the eight levels determined for the set of later experiments..

Much more experimentation should be performed on this point. It is clinically valuable to use a signal processing technique which provides reliable long term results. It would be useful to perform a set of experiments in which

the subject willfully maintains various levels of antagonist activity rather than simply relaxing his antagonist as was done in these experiments. Such a preliminary experiment has been performed involving ten second data sampling sequences for each force level in which the antagonist activity was either low, moderate or high. Although no quantitative assessment was performed, it was noted that the area encompassed by the data cluster for a force level increased greatly for higher antagonist activity.

TABLE 5.7 summarizes the results for the combined six experiments while details are presented in Fig. 5.4, 5.5 and 5.7. The number of levels with 90% confidence ($\%AVG \geq 90\%$) is also considered. Comparison of signal processing methods indicates that \overline{SUM} is still somewhat superior to \overline{RAVG} but the difference is not as distinct as was noted in Section 5.1. A degree of improvement is found using 1.0 second data windows. For a subject possessing few muscle control sites but wishing to perform many different functions, the 1.0 second window may be useful. The normalized \overline{SUM} shows an improvement over \overline{SUM} at the 95% confidence level. It may be possible with such a technique to design a processor which would provide more levels but which would require periodic calibration.

5.5 The Use of Rectangular Areas

From Section 3.3, it is clear that considerable computation is involved in determining whether or not a point

is located within an ellipse. If rectangular areas are used with the rectangle's sides oriented parallel to the BICEPS-TRICEPS axes, the computation involves only simple inequalities. This simplicity is most desirable when developing a practical processor for real time applications.

Rectangular areas were used to analyze the combined data of the six experiments performed at electrode position P_1 for method SUM using 0.5 second windows. To perform a complete analysis would have required extensive program re-writing so only two tests were conducted.

To begin, the eight force levels, which were the solution to the previously described analysis (Section 5.3) with ellipses, were considered using rectangles. With the aid of the plotting capabilities of the graphics package, the maximum value of P_{UFF} was determined such that none of the rectangles overlapped. It was discovered that for these rectangles, %AVG = 96.6% and %MIN = 92.9%. The quality of these results is comparable to that obtained using elliptical areas (Fig. 5.4(a)).

Secondly, it was found that a total of nine force levels could be defined using rectangles with %AVG = 90.8% and %MIN = 88%. These results are inferior when compared to the eleven force levels at the 90% confidence mark obtainable using ellipses.

For individuals who have difficulty in relaxing the antagonist, variation in the protagonist activity compensating for changes in the antagonist level may exist while

maintaining a constant net force. In such a case, it is expected (and has been observed in preliminary experiments) that the activities of the muscle pair increase and decrease in unison. However, this covariation should not be assumed to be linear. The use of a rectangle with sides oriented parallel to the BICEPS-TRICEPS axes would be inferior to the use of either an ellipse with its axes tilted at some angle (A_{NGL1}) relative to the coordinate system or the use of the tilted rectangle which encloses the tilted ellipse. When the data has a marked linear trait, the ellipse of minimum area was observed to be oriented so that one of its axes lay along the line of linear regression to the data. In such cases, the ellipse of minimum area had an area which was much smaller (as small as one-fifteenth) than the area of an ellipse oriented with axes parallel to the BICEPS-TRICEPS axes. In these cases, the use of non-tilted rectangles would be deleterious. The use of tilted rectangles could provide adequate results with simpler computation than required when using tilted ellipses. Further experimentation is necessary.

Although it was observed that rectangles still provide useful results, some deterioration is noted. However, it should be possible to achieve a real time processor using rectangular areas providing a reasonable level of performance, on the condition that variation in antagonist activity at a given force be small.

5.6 One-Dimensional Analysis

Many traditional methods have utilized only one EMG. To assess the performance of a one-dimensional technique, the data for the triceps signal was considered for the six experiments at electrode position P_1 using method SUM with 0.5 second windows.

Using the one-dimensional statistical parameters M_{EANT} and S_{DVT} , a procedure, analogous to the two-dimensional treatment with ellipses, was adopted. Line segments on the TRICEPS axis, representing each level, were enlarged in unison and overlapping was recorded. For each PUFF value at which line segments overlapped, the set of minimum force levels to be discarded, in order to eliminate overlap, was determined.

In this manner, five levels were defined with an average percentage of 98% of the TRICEPS values per force level lying within the bounds of the associated line segment and a minimum such percentage of 96%. Thus, only three additional distinct levels were achieved by employing the much more complex and sophisticated two-dimensional analysis in lieu of the simple one-dimensional processor.

The two-dimensional processor uses two muscles to achieve its eight levels whereas the one-dimensional processor uses only one. If a subject can be trained to use the agonists in an independent manner, it is possible that more levels could be achieved using a one-dimensional processor for each agonist. From our measurements, it was clear

that although five levels were obtainable from the triceps signal, only two additional levels could be defined for the flexors and both of these at forces in excess of 4 Kg. The reason for the poor performance with the flexor signal becomes apparent if it is recognized (Fig. 5.7) that the flexor activity during extension is not negligible. Spurious activation of the one-dimensional flexor EMG processor would occur unless only the higher levels of flexor EMG were used as controls.

CHAPTER 6

CONCLUSIONS AND SUGGESTIONS

6.1 Conclusions

A technique for the measurement and analysis of the EMG of an agonist muscle pair has been presented. It enabled the choice of both electrode position and signal processor so as to maximize the number of distinct two-dimensional areas defined within the flexor-extensor plane. The criteria for determining such regions included no overlapping between areas and a %AVG \geq 95%. Although extensive experimentation was not feasible, the data, compiled for the limited number of experiments with a single subject, yielded some useful observations.

Preliminary qualitative results revealed that for electrode position P_2 , the EMG of the flexors showed little change with wrist pronation. This suggested that one position was more favourable than the others for retrieving information concerning the contribution of the flexors to the net force. For this reason, a set of experiments was designed to quantitatively determine the effect of electrode position on the number of definable levels. It was found that electrode positions P_1 , P_2 and P_3 allowed the definition of approximately the same number of force levels. Position P_0 was

inferior. This is interesting since P_0 is the crest of the biceps muscle and is the electrode position most commonly used.

The number of definable force levels for the four electrode sites was determined using each of eleven processors. The average number of force levels for each processor was calculated and this value was used to assess the relative performance of the processors. Method $\overline{\text{SUM}}$ proved to be the superior signal processor followed closely by method SUM. The methods employing a measure of the P-P amplitude were in general superior to the power law techniques. RAVG was the best of the power law techniques examined. Electrode position P_1 in combination with method $\overline{\text{SUM}}$ provided the largest number of distinct levels (fifteen levels). More levels could be defined if 1.0 second smoothing windows were employed.

Using methods $\overline{\text{SUM}}$ and RAVG, the data for six similar experiments were analyzed to determine long-term processor performance. For both RAVG and $\overline{\text{SUM}}$ only eight levels were definable. It was postulated that the dramatic decrease in the number of definable levels, when copious data is considered, was because the agonists established a short term balance or near equilibrium muscle tension level. One measurement would then be only representative of the statistical properties of the EMG's for the particular equilibrium attained. The muscle pair could achieve the same net force by using any of the numerous combinations of agonist tension. It was observed that data for different experiments and even

data for different sampling sequences within a single experiment could be clustered in very distinct areas. This observation supported the concept of agonist equilibrium during a sampling sequence.

Another reason for the great reduction in the number of levels when data is combined from several experiments could be the day to day emotional and physiological state of the subject. The variation in the subject's emotional or physiological state may effect his controllability of the antagonist activity and it's fluctuations even though net force may be controllable. Since the agonists assume near equilibrium during any one measurement, it is absolutely essential to consider a large number of measurements to obtain an accurate representation of the statistical variations. Experimenters must be cautious when drawing conclusions from limited data.

Dorcas et al [8] [9] found that three levels could be established using one muscle site. If the agonists could be used independently, a total of six levels could be defined in comparison with the eight levels in this analysis. We observed that the antagonist is usually quite active and in practice, it may be difficult to use the two agonists for separate control signals. The subject would also be required to develop the skill of using the agonists in an independent fashion. We considered a simple one-dimensional controller for the extensor EMG that permitted five levels. If the extensor was used in this manner, problems arose when attempting

to use the flexor for a separate control signal. With the flexor as the protagonist unwanted triggering of the extensor processor could occur. This triggering could be due to cross talk of muscle EMG or due to an intrinsic level of antagonist activity which is a function of protagonist tension.

The number of definable force levels considering the combined data for six experiments was found using 1.0 second windows. SUM provided ten levels while RAVG allowed nine. The lengthening of the window has the disadvantage that system response is more sluggish.

A primitive normalization scheme was also tested on method SUM and an improvement from eight to ten levels was found when using 0.5 second windows. Although normalization is promising, some additional computation is required.

When the data for three different electrode positions was considered, a combined total of ten levels was achieved using SUM with 0.5 second windows. This indicates that the magnitude of the means of the DISTILLED data are approximately constant over a wide area and by using these techniques, it may be possible to design a signal processor which is relatively insensitive to electrode placement.

The use of SNR to assess the relative performance of processors was found to produce results inconsistent with those obtained using the number of definable force levels as a figure of merit. Since SNR does not contain information concerning the signal processor's sensitivity to changes in

the EMG, it is considered to be a poor parameter with which to assess performance.

6.2 Suggestions for Further Work

Many more experiments should be performed to acquire an extensive data base. The effect of electrode position should be studied for both agonists. The relative performance of processors should be assessed for a large number of experiments. Many individuals should be studied to determine if there is any pattern relating the superior processor and electrode position to the individual's physiology. If a grid of surface electrodes were placed over the arm and the signals from all electrodes were sampled and stored simultaneously, analysis of the samples would provide a useful technique for studying the effect of electrode position since uniform conditions would prevail.

It is felt that the experimental procedure and the electronics presented provide adequate signal integrity when the arm is stationary. For the moving arm, a different electrode scheme may be necessary to reduce motion artifacts. Further miniaturization of the source attached amplifiers is necessary. It is estimated that the amplifier volume could be reduced by 50% or more with the current design but further reduction would require the design of an integrated circuit without external components. By using the chip for the instrumentation amplifier which we employed, a hybrid circuit could easily be realized that would be most effective.

In retrospect, it is felt that some of the analysis techniques employed were unnecessarily complex. Rather than allow all ellipses to enlarge in unison, it would have been simpler, and superior from the point of view of realizing more levels, to determine the enlargement factor necessary for each ellipse to envelope 95% of the DISTILLED data points. Overlapping ellipses could then be discarded so that the maximum number of distinct ellipses remain. Future efforts which employ the same methods which we did could improve on them by choosing the best of all the available sets of minimum elements. The best set could be chosen as the one which maximizes %AVG.

Although the use of rectangles, with sides parallel to the flexor-extensor axis, provided eight levels from the combined data of six experiments, it is felt that they would provide poor results in the situation where the protagonist activity varies. A study of the performance of "tilted" rectangles enclosing the solution ellipses should be made.

Both methods SUFF and RAVG could easily be realized employing one of the many currently available microprocessors. The greatest drawback in the use of the ellipse is that determining whether or not a point lies within an ellipse involves time consuming multiplication. The use of a microprocessor with interrupt capability would allow such lengthy calculations to be performed periodically with simultaneous signal sampling. If necessary, a currently available microprocessor performing rapid multiplication (17 μ s) or a one chip

multiplying unit (300 ns) could be used. If tilted, or better still, non-tilted rectangular areas were adequate, the determination of whether or not a point is lying within a certain region would be extremely simple. Using rectangular areas, a large number of agonists could be monitored using one microprocessor, thereby achieving good performance/weight, performance/cost and performance/bulk ratios.

Another desirable feature for signal processing would be the use of sliding windows which slide by perhaps 0.1 seconds. In using these windows, $\overline{\text{SUM}}$ or RAVG methods would be evaluated for each 0.1 second interval and the data stored to be used in calculating $\overline{\text{SUM}}$ or RAVG over the entire 0.5 second window. It would therefore be necessary to store five such values for each EMG at any one time. This would only slightly increase the random access memory requirements of the system and provide a more responsive controller.

RAVG has the advantage that it may be realized using analog components. If it is desired to monitor the activity from a large number of agonists, analog processors could be used to determine the rectified average for each muscle. The microprocessor could sample the outputs of this large number of analog processors at a low sampling rate. It may, however, prove to be more desirable to use more than one processor to perform the task rather than resort to a large number of analog modules.

Throughout these experiments, the subject maintained the desired constant force levels with the elbow resting on a pad, supporting a fraction of the upper body weight. In this configuration, agonist muscle activity, for a given net force, can vary due to reaction force (Milner, private communication (24)). Simply by exerting the desired force with the arm hanging from the shoulder rather than supported at the elbow, much of the postural effect due to reaction force is eliminated. Since this was not done in our experimentation, the varying reaction force is another possible cause of the deterioration observed in our results when the data for many ten second sampling intervals (each interval with perhaps a different reaction force) were combined. It is suggested that this factor be considered when designing future similar experiments.



REFERENCES

- [1] B. Katz, Nerve Muscle and Synapse, McGraw-Hill Book Company, (1966).
- [2] H.S. Milner-Brown and R.B. Stein, "The Relation Between the Surface Electromyogram and Muscular Force", J. Physiol., (Lond.), vol. 246, (1975), pp. 549-569.
- [3] R. Fuschfeld, "Analysis of Electromyographic Signals By Measurement of Wave Duration", Electroencephalogr. Clin. Neurophysiol., vol. 30, (1971), pp. 337-344.
- [4] H. deBruin, Dept. of Elec. Engr., McMaster University.
- [5] J.G. Kreifeldt and Sumner Yao, "A Signal-to-Noise Investigation of Nonlinear Electromyographic Processors", IEEE Trans. Bio-Med. Eng., vol. BME-21, no. 4, (July 1974), pp. 298-308.
- [6] P.D. Neilson, "Speed of Response or Bandwidth of Voluntary System Controlling Elbow Position in Intact Man", Med. Biol. Eng., vol. 10, (1972), pp. 450-459.
- [7] J.G. Kreifeldt, "Signal versus Noise Characteristics of Filtered EMG Used as a Control Source", IEEE Trans. Bio-Med. Eng., vol. BME-18, no. 1, (January 1971), pp. 16-22.
- [8] D.S. Dorcas and R.N. Scott, "A Three-State Myo-Electric Control", Med. Biol. Eng., vol. 4, (1966), pp. 367-370.
- [9] D.S. Dorcas, V.A. Dunfield and R.N. Scott, "Improved Myo-Electric Control System", Med. Biol. Eng., vol. 8, (1970), pp. 333-341.
- [10] A.H. Bottomley, "Myo-Electric Control of Powered Prosthesis", J. Bone Joint Surg., vol. 47-B (1965), pp. 411-414.
- [11] M.J. Hall and T.H. Lambert, "The Use of Muscle Electric Potential for the Position Control of Artificial Arms",

- Proc. Inst. Mech. Eng., (London), vol. 183, (1968-69), pp. 103-108.
- [12] T.H. Wonnacott and R.J. Wonnacott, Introductory Statistics, J. Wiley & Sons, Inc., (1972), pp. 59-82.
- [13] J.V. Basmajian, Muscles Alive, Williams & Wilkins, (1967), pp. 172-178.
- [14] D. Graupe and W.K. Cline, "Functional Separation of EMG Signals via ARMA Identification Methods for Prosthesis Control Purposes", IEEE Trans. Syst. Man Cybern., vol. SMC-5, no. 2, (March 1975), pp. 252-258.
- [15] B.H. Brown, "Waveform Analysis of Surface Electrode EMG's Used to Give Independent Control Signals from Adjacent Muscles", Med. Biol. Eng., vol. 6, (1968), pp. 653-658.
- [16] J. Whitman, SOC Report #127, July 1976.
- [17] R.L. Burford, Statistics: A Computer Approach, Charles E. Merrill Publishing Co., (1968), pp. 23-59.
- [18] L.A. Geddes, R. Steinberg and G. Wise, "Dry Electrodes and Holder for Electro-Oculography", Med. Biol. Eng., vol. 11, (1973), pp. 69-72.
- [19] E. Kwatny, D.H. Thomas and H.G. Kwatny, "An Application of Signal Processing Techniques to the Study of Myoelectric Signals", IEEE Trans. Bio-Med. Eng., vol. BME-17, no. 4, (October 1970), pp. 303-312.
- [20] J.V. Basmajian and J.E. Hudson, "Miniature Source-Attached Differential Amplifier for Electromyography", Am. J. Phys. Med., vol. 53, no. 5, (1974), pp. 234-236.
- [21] A. Kamp, H.L. Kok and F.W. deQuartel, "A Multiwire Cable for Recording from Moving Subjects", Electroencephalogr. Clin. Neurophysiol., vol. 18, (1965), pp. 522-423.
- [22] P.D. Neilson, "Frequency-Response Characteristics of

the Tonic Stretch Reflexes of Biceps Brachii Muscle
in Intact Man", Med. Biol. Eng., vol. 10, (1972),
pp. 460-472.

(23) Opcit, J.V. Basmajian, Muscles Alive, pp. 131-135.

(24) M. Milner, Dept. of Elec. Engn., McMaster University.